Atmospheric Research

Intrusions of dust and iberulites in Granada basin (Southern Iberian Peninsula). Genesis and formation of atmospheric iberulites

--Manuscript Draft--

Manuscript Number:	ATMOSRES_2020_228R2
Article Type:	Research Paper
Section/Category:	Aerosol particles
Keywords:	Rare Earth Elements; Saharan dust; Iberulites genesis; Bacterial EPS; Human health
Corresponding Author:	Alberto Molinero-García Universidad de Granada (Departamento de Edafología y Química Agrícola) Granada, Spain Spain
First Author:	Jesús Francisco Párraga-Martínez
Order of Authors:	Jesús Francisco Párraga-Martínez
	Alberto Molinero-García
	Juan Manuel Martin-Garcia
	Gabriel Delgado Calvo-Flores
	Ana Cervera-Mata
	Isabel Guerra
	María Virginia Fernández-González
	Francisco Javier Martín-Rodríguez
	Hassan Lyamani
	Juan Andrés Casquero-Vera
	Antonio Valenzuela Gutierrez
	Francisco Jose Olmo Reyes
	Rafael Delgado
Abstract:	Fourteen samples of deposited atmospheric dust collected during desert dust intrusions over Granada in the summer of 2010 are studied here. During these atmospheric dust events the PM10 ranged from 25 µg m-3 to 200 µg m-3, surpassing occasionally the standard limit (50 µg m-3) established by the European Union Directive as a risk for the human health. The mineralogical composition of the dust samples is very heterogeneous, showing that the origin of collected particles is from north-northwest of Africa and local/regional soils. The analyzed dust samples contain between 1 and 9% of iberulites, polymineral spherical particles with diameter between 34 and 111 µm. New compositional results obtained by mapping chemical elements and mineral compositions of Iberulites with VPSEM-EDEX technology allowed as to go further than previous studies and provide new insight on the iberulites genesis. The SEM-microstructure analysis of the iberulites and the compositional results obtained by VPSEM-EDEX technique showed that clay and Sulphur components are important in determining their spherical shapes. The analysis also shows that iberulites present a typical vortex at one of the poles and an external covering by nano-clays in laminar clusters, a form of rind and a core internal with sizes less than 10 microns. On the other hand, the micromorphological analysis evidences that the bacteria and its polymeric exudates participate in the iberulite genesis, acting as aggregation agents and contributing to its protection and compensating its fragility. The role of bacteria and its polymeric exudates in the iberulite genesis has not been described previously, and it would explain the flux, transport and survival of tropospheric microorganisms over long distances. These new observations and finding led us to take into account the role of bacteria in iberulite genesis and to reconsider the previous hypothesis regarding the iberulite genesis proposed in previous works.

Suggested Reviewers:	Celia Alves celia.alves@ua.pt She is an expert in atmospheric processes, air quality and aerosols
	Ana Isabel Calvo aicalg@unileon.es She is an expert both in atmospheric chemistry and to caracterize atmospheric aerosols
	Andres Alastuey andres.alastuey@idaea.csic.es He is an expert in environmental geochemistry and air pollution. He has focused on the geochemistry of atmospheric aerosols because of its impact on air quality, human and health.
	Javier Cuadros j.cuadros@nhm.ac.uk He is an expert in mineralogy and geochemistry
	Dirk Scheuvens dscheuvens@geo.tu-darmstadt.de He is and expert in mineralogy and air quality
Response to Reviewers:	

Editor-in-Chief

Atmospheric Research

Dear Editor:

Please find enclosed the manuscript entitled "Genesis and provenance of atmospheric iberulites in Granada basin (Southern Iberian Peninsula)" to be considered for publication in Atmospheric Research.

The manuscript fits the aims and scope of this journal since it deals with “Air pollution”, in particular with a topic of large interest for the scientific community as well as for policy makers since better understanding on the Iberulites (a new type of spherical aerosol giant particle), and its composition, origin and the potential to affect health and ecosystems. Whereas some papers have studied the iberulites (origin and compositions), in this work we analyzed: 1) the mineralogical composition, including some particular results, and compared with other reported studies; 2) the REE composition, which has not yet been studied during African dust intrusions over southern Spain; 3) the identification of source regions of sedimentable mineral dust using mineralogy and REE as fingerprints of provenance; 4) the analysis of their genesis by bacterial mechanisms, not studied previously; 5) its high porosity permits them to stay for a long time in the atmosphere and to behave as intercontinental vehicle (“shuttles”) for the transport and survival of microorganisms.

Such a methodologically complete and multidisciplinary approach, with novel objectives, has not been attempted to date.

In our future studies, we will investigate types of microorganisms carried by the dust.

Thank you very much for your attention.

Yours sincerely,

Alberto Molinero-García

University of Granada

Review of "Intrusions of dust and iberulites in Granada basin (Southern Iberian Peninsula). Genesis and formation of atmospheric iberulites" by Párraga et al.

We would like to express again our sincere gratitude to reviewers for their comments. We believe that the paper has improved with this modifications. Hereafter, our answers to reviewers are shown in bold.

Reviewer #2 (blue):

Authors responded the comments well, they have shorten section 3.3 and 3.4 and revised the title of the paper so that it reads clear and close to the main contents.

I have only one suggestion for the item #3 of highlights, namely "New insight on the iberulites genesis due to both elements and mineral distribution", this sentence is not informative, it would be better to state what kind of new insight on the iberulites genesis is obtained from this research, or alternatively, this item can be deleted because the latter two items did provide the "new findings" of the study.

We agree and following the reviewer suggestions, we have removed the item #3 of highlights: "New insight on the iberulites genesis due to both elements and mineral distribution".

Highlights:

- Iberulite, microspherulite with vortex, both mineral and microorganisms assemblage.
- The Clay and the S components are decisive in Iberulites spherical shape.
- Bacteria act as an aggregation agent for Iberulites.
- Micromorphological evidences the bacteria implication in the iberulite genesis.

Graphical Abstract Click here to access/download;Graphical Abstract;Parraga et al Graphical Abstract.tif

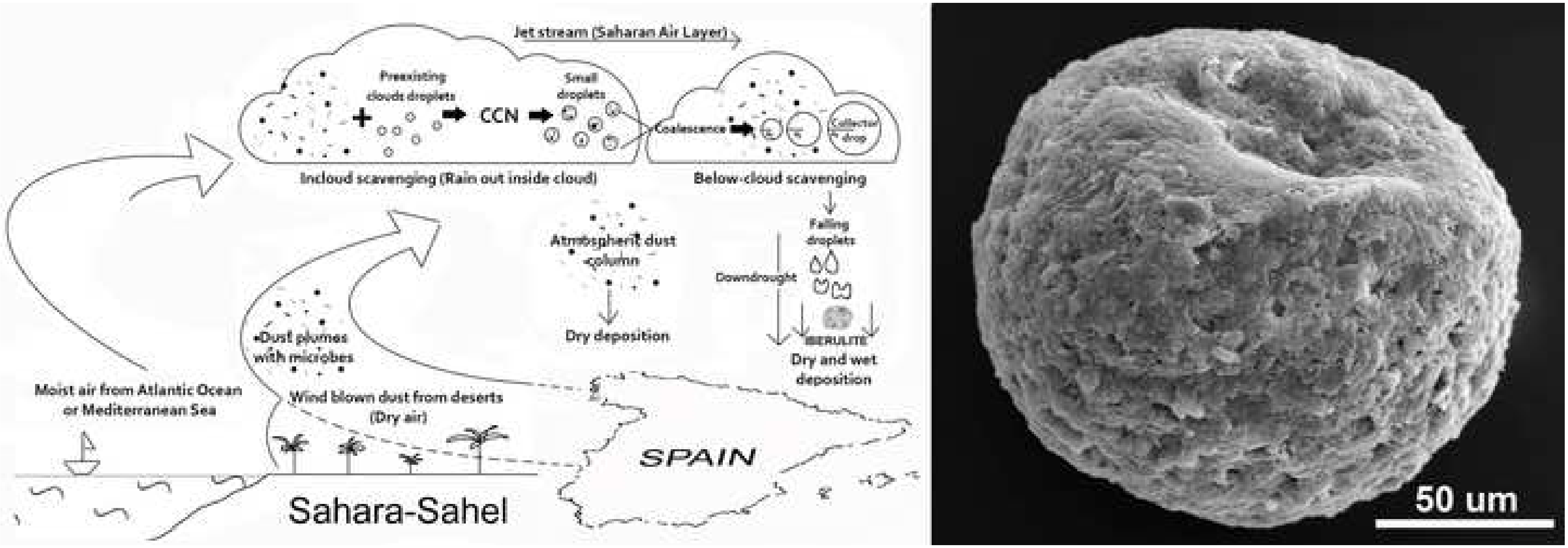

Intrusions of dust and iberulites in Granada basin (Southern Iberian Peninsula). Genesis and formation of atmospheric iberulites

J. Párraga[a], J.M. Martín-García[a], G. Delgado[a], A. Molinero-García[a]*, A. Cervera-Mata[a], I. Guerra[b], M.V. Fernández-González[a], F.J. Martín-Rodríguez[a], H. Lyamani[c,d], J.A. Casquero-Vera[c,d], A. Valenzuela[c,d], F.J. Olmo[c,d] and R. Delgado[a]

[a] Department of Soil Science and Agriculture Chemistry. Faculty of Pharmacy, University of Granada.

[b] Unidad de Microscopía Electrónica de Barrido de alta resolución y Microanálisis. Centro de Instrumentación Científica.

[c] Andalusian Institute for Earth System Research, IISTA-CEAMA, University of Granada, Junta de Andalucía, Granada 18006, Spain

[d] Department of Applied Physics, University of Granada, Granada 18071, Spain

***Author for correspondence. Email: amolinerogarcia@ugr.es**

Abstract:

Fourteen samples of deposited atmospheric dust collected during desert dust intrusions over Granada in the summer of 2010 are studied here. During these atmospheric dust events the PM10 ranged from 25 µg m^{-3} to 200 µg m^{-3}, surpassing occasionally the standard limit (50 µg m^{-3}) established by the European Union Directive as a risk for the human health. The mineralogical composition of the dust samples is very heterogeneous, showing that the origin of collected particles is from north-northwest of Africa and local/regional soils. The analyzed dust samples contain between 1 and 9% of iberulites, polymineral spherical particles with diameter between 34 and 111 μm. New compositional results obtained by mapping chemical elements and mineral compositions of iberulites with VPSEM-EDEX technology allowed as to go further than previous studies and provide new insight on the iberulites genesis. The SEM-microstructure analysis of the iberulites and the compositional results obtained by VPSEM-EDEX technique showed that clay and sulphur components are important in determining their spherical shapes. The analysis also shows that iberulites present a typical vortex at one of the poles and an external covering by nano-clays in laminar clusters, a form of rind and a core internal with sizes less than 10 microns. On the other hand, the micromorphological analysis evidences that the bacteria and its polymeric exudates participate in the iberulite genesis, acting as aggregation agents and contributing to its protection and compensating its fragility. The role of bacteria and its polymeric exudates in the iberulite genesis has not been described previously, and it would explain the flux, transport and survival of tropospheric microorganisms over long distances. These new observations and finding led us to take into account the role of bacteria in iberulite genesis and to reconsider the previous hypothesis regarding the iberulite genesis proposed in previous works.

Keywords: Saharan dust; Iberulites genesis; Rare Earth Elements; Bacterial EPS; Human Health.

Highlights:

- Iberulite, microspherulite with vortex, both mineral and microorganisms assemblage.
- The Clay and the S components are decisive in Iberulites spherical shape.
- Bacteria act as an aggregation agent for Iberulites.
- Micromorphological evidences the bacteria implication in the iberulite genesis.

Graphical Abstract:

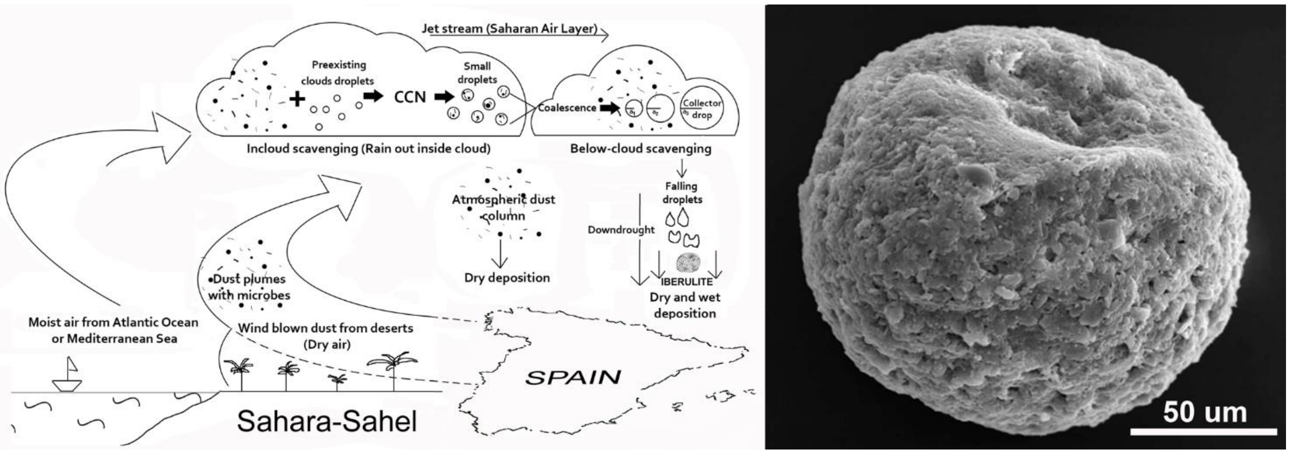

Sequence of iberulite formation vía “cloud processing” with bacterial activity

1. Introduction

Every year between 1 and 3 billion tons of dust are emitted into the atmosphere from arid and semi-arid areas, particularly from the Sahara and Sahel (North Africa), which are responsible for 50-70% of the global dust emissions. Due to its proximity to the African continent, the Iberian Peninsula is frequently affected by desert dust intrusions, especially in the summer season (e.g., Valenzuela et al., 2012a). This dust intrusion phenomenon also affects a large area of Europe, with annual dust mass concentrations between 80 and 120 Tg (e.g., Pey et al., 2013).

During major dust intrusions from North Africa the concentrations of PM10 (particles with an aerodynamic diameter < 10 μm) often exceed the European PM10 air quality standard limits in different European countries (Rodriguez et al., 2001; Reyes et al., 2014), negatively affecting public health (Varga et al., 2014; Oduber et al., 2019). In addition to the effects on human and animal health, the mineral dust also affects climate and ecosystems (e.g., Jeong et al., 2016).

In order to better understand the effects of the dust on climate, atmospheric chemistry, biogeochemical cycles and primary biological production more dust mineralogical studies are still needed (e.g., Engelbrecht et al., 2016). In this sense, the aerosol mineralogy is a difficult property to study due to the difficulties inherent in studying very small objects, such as dust particles, using highly specific techniques including Scanning Electron Microscopy (SEM), Trasmisision Electron Microscopy (TEM) and Energy Dispersive X-Ray Spectroscopy (EDX).

On the other hand, the study of the geographical origin of atmospheric dust is an innovative topic of great interest. Scheuvens et al. (2013) used the mineralogical composition of African dust to detect the origin of transported dust. The rare earth elements (REE: lanthanides and yttrium) are also good dust tracers of geochemical processes and dust origin as they are closely related to the materials of the source area (e.g., Wang et al., 2017). However, there are few REE studies of the atmospheric dust deposited in the Iberian Peninsula. Another method most frequently employed by the scientific community to determine the origin of desert dust is that based on the analysis of the back-trajectories of air masses (e.g., Lyamani et al., 2005; Valenzuela et al., 2012a).

The atmospheric African dust reaching Spain contains up to 47% of giant polymineral particles with diameters between 50 and 200 µm, generated by atmospheric aggregation. These particles were named iberulites by Díaz-Hernández and Párraga (2008). Iberulites were observed in Mallorca (Spain) by Fiol et al. (2001, 2005) and in Tenerife (Canary Islands, Spain) by Cuadros et al. (2015). Furthermore, Iberulites were also observed in atmospheric air masses from Saudi Arabia (Posfai et al., 2013) and in Volgograd (Russia) (Kuzmichev et al., 2017). The potential of iberulites to adversely affect human/animals health is due to the fact that they are constituted by potentially harmful micro- and nanometric breathable particles (Vahlsing and Smith, 2012) and they are able to transport biological materials, thus converting them into potential vehicles for pathological infections of humans and animals (Párraga et al., 2013). The microstructure of these aeolian particles is closely related to their genesis in the atmosphere and to processes occurring when they fall to the ground (Díaz-Hernández and Párraga, 2008; Jeong and Nousiainen, 2014; Jeong et al., 2014; Díaz-Hernández and Sánchez-Navas, 2016). Until now, there is little knowledge about the transformation processes as well as about mineralogical and biological compositions of iberulites and, therefore, more studies are needed to improve our knowledge about them.

The main aim of the present work is to explore the mineralogical composition of deposited atmospheric aerosol particles during African dust intrusions over the city of Granada (Spain). We will also study their REE composition, which has not yet been studied during atmospheric dust intrusions over southern Spain. In addition, special emphasis will be put on the identification of source regions of deposited mineral dust using mineralogy and REE composition as well as air mass back-trajectories. Finally, we will study the iberulites during the African dust events and their genesis by bacterial mechanisms, not studied previously.

2. Sampling and methods

2.1 Sampling site

Experimental measurements were obtained in the metropolitan area of Granada (37º 08' 59" N, 03º 37' 59" W, 650 m a.s.l.). Granada is a non-industrialized Spanish city with a population of about 250.000, located in the southern Iberian Peninsula, around 50 km from the Mediterranean Sea. Climate is semi-arid to dry ombrotype and meso-Mediterranean thermotype with marked cycles of drought and precipitation every 5 to 10 years. Granada is situated in a natural basin surrounded by mountains (1000 - 3398 m a.s.l.) of siliceous dolomitic limestone. Soils are mainly calcareous Fluvisols, under irrigation or dedicated to olive groves. Due to its proximity to the African continent, Granada is frequently affected by Saharan dust intrusions. The number of African dust intrusions is quite high, especially during summer, with a frequency up to 45% of the days in June-August (e.g., Valenzuela et al., 2012b). Usually, mineral dust particles are transported over Granada at high altitudes of up to 5500 m a.s.l. However, in some cases African dust reaches surface ground level due to dry or wet deposition (e.g., Calvo et al., 2010). The local aerosol sources are mainly the heavy traffic, the domestic heating and the re-suspension of material available on the ground, especially during warm season. The reduced rainfall and the dryness of the terrain can increase the contribution of local mineral dust (e.g., Lyamani et al., 2010).

2.2. Collection of dust, iberulite and soil samples

The sampling station, with collectors of deposited atmospheric dust (DAD) by dry deposition, was located on the roof terrace of a building some 10 m above the ground on a mast 2 m higher than the terrace (Díaz-Hernández and Parraga, 2008). The terrace was covered with coarse gravel (20-40 mm diameter), which, to a large extent, prevent the resuspension of the dust deposited there. The station has been in operation since 2004. Sampling was carried out weekly. Deposited dust concentration was determined by weight. In the present study, 14 DAD samples collected during atmospheric dust intrusions over Granada in the summer of 2010 are analyzed in more detail (Table 1). It should be noted that we opted to analyze DAD samples from the summer of 2010 because this year was the year with the most dust intrusions in the southern Iberian Peninsula, according to the CALIMA network (www.calima.ws/2010.pdf).

The quantity and size of iberulites (Table 1) were estimated from digital images (program Analysis-getIT), counting around 500 dust particles from each sample. These particles were isolated from the fine fraction (<200 μm) (obtained by sieving the dust) in the object field of a stereomicroscope (Olympus B061) using a sleeved needle.

In order to study bacteria, soil samples (calcareous Fluvisol) were collected during summer 2010 close to the station (37.15º N, 3.63º W) with horizon Ap (0-20 cm) being selected. For the mean mineralogical compositions of the most common soils in Granada we used the data reported by Márquez (2012), who studied a soil of the same type and close to our studied soil, with an Ap horizon of sandy loamy texture (35.6% sand, 47.8% silt and 16.6% clay), 1.70% organic carbon, 0.19% N, pH (water) 7.3, 21% $CaCO_3$ and totally saturated in exchange cations.

2.3. Suspended particulate matter

The measurements of the concentration (in μg m^{-3}) of atmospheric particulate matter PM10 were taken at the EMEP (cooperative programme for the monitoring and evaluation of the long range transmission of air pollutants in Europe) background station in Viznar, 10 km from the city. The PM10 dataset registered at this background station are very useful for the detection of long range transported aerosol particles such as Saharan mineral dust. Also, these data can give us more insight about the impact of the different African dust intrusions on background aerosol concentration over Granada metropolitan area. As the station is an EMEP station, site selection criteria, sampling, analysis and data quality control protocols are pre-established (EMEP, 2001).

2.4. Methodology. Analysis of deposited dust and iberulites

A more detailed description of the sampling methodology, sample treatment and analytical procedures used here is given by Díaz-Hernández and Párraga (2008) and Párraga et al. (2013). A brief description of the methods and instrumentation used in this study is provided here. In this work we also included new analytical methods for the determination of some REE contents and news in the study of the mineralogical composition by X-ray diffraction (XRD) and Electron Microscopy techniques.

The size distribution of particles collected in DAD samples was obtained by Wet dispersion laser diffraction (Mastersizer 2000, Malvern Instruments Ltd., UK). For the analysis of the mineralogical composition of DAD samples we used XRD technique. The diffraction patterns were obtained by Brucker AXS D8 ADVANCE instrument using Cu Kα radiation by continuous scan between 3 and 70º 2θ with velocity of 2º min^{-1}. The obtained diffractograms were interpreted using the XPowder Program (Martín, 2004). Percentages of mineral contents were estimated using intensity factors of Schultz (1964), Barahona (1974) and Delgado et al. (1982). The presence of palygorskite was investigated with the peak at 0.63 nm (basal distances d_{200}; 15% intensity). For identification of dust origin the obtained mineral compositions are presented in the triangle Carbonates (calcite + dolomite) – Tectosilicates (quartz + K-feldspar + plagioclases) – Phylllosilicates + Fe oxides (hematite + goethite) (Calero et al., 2009).

On other hand, the REE contents in DAD samples were determined by ICP-MS method (inductively coupled plasma mass spectrometry) with quadrupole ion filter ICPMS NEXION 300D PERKIN-ELMER, USA. For ICP-MS analysis, the collected samples were previously disaggregated in HNO_3 and HF. The REE were grouped into: Light (LREE: La, Ce, Pr, Nd), Medium (MREE: Sm, Eu, Gd, Tb, Dy) and Heavy REE (HREE: Ho, Er, Tm, Yb, Lu). Note that Y was not considered in this classification. REE concentrations were chondrite-normalized (using standard CI chondrite of McDonough and Sun, 1995), with Y represented between Ho and Er (Korotev, 2009). After that, we calculated the geochemical indices $HREE_N/LREE_N$ and $MREE_N/LREE_N$ and the anomalies Ce/Ce*, Eu/Eu* and Y/Y* ($Ce/Ce^* = Ce_N/(La_N \times Pr_N)^{1/2}$; $Eu/Eu^* = Eu_N/(Sm_N \times Gd_N)^{1/2}$; $Y/Y^* = Y_N/(Ho_N \times Er_N)^{1/2}$, where the suffix "N" indicates that the chondrite-normalized value was used) (Mourier et al., 2008; Laveuf and Cornu, 2009).

For the analysis of the morphology (external morphology and internal microstructure) and elemental composition of iberulites collected in DAD samples we used Scanning electron microscopy (secondary and backscattered electrons) and electron microanalysis methods (SEM Hitachi S-510, VPSEM Zeiss SUPRA40VP and Rontec–EDX) as well as image analysis (IA). For VPSEM-EDX mapping, the DAD samples were embedded in Epon resin and the iberulites were cut with a diamond microtome to expose their interiors. The mineralogical compositions of these cut iberulites were determined using maps of chemical elements by comparisons with mineral standards. For thin sections (70-90 nm) of iberulites, high resolution transmission electron microscopy (HRTEM) technique was used (STEM PHILIPS CM20, Holland). For VPSEM observation of bacteria in deposited dust samples, iberulites and soil, the samples were first fixed with 2.5% glutaraldehyde in 0.1 M cacodylate buffer, and subsequently fixed with 1% osmium tetroxide, dehydrated with alcohol, dried using the critical point method and finally they were coated with carbon (Kuo, 2007). Other samples were simply covered with carbon.

All equipment detailed in this section belongs to Centro de Instrumentación Científica (CIC), University of Granada.

2.5 Detection of desert dust events and identification of their origin

For detecting the African desert dust intrusions over the Iberian Peninsula, CALIMA uses the models SKIRON, BSC-DREAM, NAAPs and HYSPLIT4 backtrajectory analyses (Draxler et al., 2003), as well as synoptic meteorological charts, satellite images, and surface data (particulate matter recorded at air quality monitoring background stations). The air mass backward trajectories calculated by HYSPLIT were used to detect the source regions of desert dust observed over our study area during 2010 by the method described by Valenzuela et al. (2012b). This method assumes that the dust particles are confined to the mixed layer at the potential source region, and that the air mass is loaded by desert dust when the air mass altitude is lower than or close to the altitude of the mixed layer at potential source.

3. Results and discussion

3.1 Concentrations of PM10

The evolution of mean daily concentrations of atmospheric PM10 during the study period is shown in Fig. 1. These atmospheric PM10 concentrations ranged from 25 µg m^{-3} to 200 µg m^{-3} during the analysed period. Some PM10 concentrations were greater than 50 µg m^{-3}, the standard limit established by the European Union Directive (2008/50/EC). The highest PM10 values were observed from 7^{th} to 13^{th} August, reaching the maximum value of 200 µg m^{-3} on 10 August. African dust intrusions are common in the Granada basin between May and October, although there may also be events in February-March (Rodriguez et al., 2001; De la Rosa et al., 2010; Valenzuela et al., 2012b). Fourteen desert dust intrusions over our study area during the summer 2010 have been confirmed by the CALIMA network (www.calima.ws). In fact, high PM10 values observed during the analyzed period were associated with Saharan Dust Outbreaks (shaded areas in Fig. 1b) as confirmed by CALIMA (www.calima.ws). According to the CALIMA network, 2010 was the year with the greatest number of Saharan Dust events, with 32 dust events, during the period 2004-2015. The total number of Saharan Dust events in the southeast of the Iberian Peninsula between 2004 and

2016 was 314 African dust intrusions, giving 1349 days of Saharan events (www.calima.ws). In addition, the air mass backward trajectories calculated by HYSPLIT show that the source regions of desert dust at our study area during the summer 2010 were Western Sahara, northwestern Mauritania and southwestern Algeria.

3.2 Deposition and granulometry analyses of deposited dust and iberulites

The deposition rate (Fig. 1) shows a high variability ranging from 23 mg m^{-2} day^{-1} (for JP01 sample) to 168 mg m^{-2} day^{-1} (for JP04 sample). The mean deposition rate was 57 mg m^{-2} day^{-1} during the analyzed period. As can be seen, high deposition rates were registered in July-August and low ones in June and last October. No direct relationship could be observed between PM10 concentration (Fig. 1b) and deposition rate (Fig. 1a), since PM10 concentration only include particles with diameter lower than 10 μm and collected samples include particles with size larger than 10 μm. In fact, the maximum deposition rate was observed during 21-27 July while the highest PM10 concentration was registered from 6 to 13 August 2010.

The collected deposited dust consisted mainly of particles with diameter less than 200 µm (mean = 92.3%) (Table 1). Particles with diameter between 200 and 500 µm represented 5.8% (on average) of the total volume concentration, while those of diameter greater than 500 µm only accounted for 2% of the total concentration. The data from Table 1 show that the granulometry presents a small variation between dust events (coefficient of variation <200 µm = 3.4%). However, some selected granulometric curves (Fig. S1) show that, although the mean size is always fine sand (between 50 and 200 µm) the mean size values are relatively different (between 51.79 µm for JP04 sample and 100.31 µm for JP08 sample).

In all 14 dust samples analyzed, iberulites were found. However, the quantity of iberulites as a percentage of the total dust sample mass concentration varied considerably (coefficient of variation = 88.5%), from very low (0.7% in JP13 sample) to a more elevated contribution (9.2 % in JP02 sample), with a mean value of 2.6% (Table 1). The mass fractions of iberulites obtained in this study are much lower than those observed in the same study zone in 2001 and 2005, which ranged from 16 to 47% (Díaz-Hernández and Párraga 2008).

The mean apparent diameter of the iberulites collected was also variable, varying from 34 µm (sample JP10) to 111 µm (sample JP14), with a mean value of 61 µm (coefficient of variation = 32.8%). Electron microscopy analysis confirmed these measurements (see the corresponding section), and also showed that the constituent particles of the iberulites can reach sizes smaller than 1 µm. The mean diameter of the iberulites obtained in this study (61 µm) differs from that reported by Díaz-Hernández and Párraga (2008), 90 µm, and is in the size range (40 - 300 µm) reported by Fiol et al. (2001, 2005).

3.3 Mineralogical analyses of dust samples

The mineralogical composition of the DAD analyzed in this study is very heterogeneous (Table 2). These mineral phases are usually found in the dust samples previously studied in Granada and its metropolitan area (Díaz-Hernández and Párraga, 2008; Díaz-Hernández et al., 2011; Rodríguez-Navarro et al., 2018), and in other locations in the Iberian Penninsula and Balearic Islands (Queralt et al., 1993; Ávila et al., 1997; Fiol et al., 2001, 2005; Fornós et al., 2004). However, palygorskite, detected in African dust over Iberian Peninsula by Queralt et al. (1993), Ávila et al. (1997), Fiol et al. (2005), Fornós et al. (2004), Díaz-Hernández et al., (2011) and Rodríguez-Navarro et al. (2018) (Table 3) was not detected in the dust samples studied here by XRD nor by VPSEM-EDX method (see the corresponding section).

The mineral composition is variable (Table 2), dominated by phyllosilicates, quartz and dolomite. Gypsum presented very low content (<3 %), possibly as an atmospheric neoformation product of the attack of atmospheric H_2SO_4 on some primary minerals as smectites and calcite (Díaz-Hernández and Párraga, 2008).

Due to the small quantities collected in dust samples, iberulites could not be analysed by XRD. However, the mineral composition of iberulites reminds the composition of the dust, according to the results from electron microscopy and microanalysis (see Section 3-5).

In the triangle Carbonates – Tectosilicates – Phylllosilicates + Fe oxides (Fig. 2) the samples studied here occupy a relatively small zone, characterized by higher contents of Phyllosilicates + Iron forms and a composition of Carbonates and Tectosilicates that maintain their relative proportions, except for JP08 sample, which was rich in Tectosilicates. When atmospheric dust samples from the bibliography (Queralt et al., 1993; Ávila et al., 1997; Fiol et al., 2001, 2005; Formós et al., 2004; Díaz-Hernández y Párraga, 2008; Díaz-Hernández et al., 2011; Rodríguez-Navarro et al., 2018) as well as the data of the regional soils (Sierra Nevada, Sierra Gádor and Granada) (Delgado et al., 2003; Martín-García et al., 2004; Márquez, 2012) are also considered, the following finding can be highlighted (Fig. 2):

1) Mineral composition of the different dust samples shows a large dispersion, although always below the line of 55% carbonates, which again evidence the mineral heterogeneity of the atmospheric dust samples. However, it cannot be discarded that the different methods used for mineral composition analysis (Table 3) could contribute to this dispersion. Ávila et al. (1997) and Queralt et al. (1993) applied XRD-Chung's method, Díaz Hernández and Párraga (2008) employed X Powder-RIR method, Fiol et al. (2005) and Fornós et al. (2004) used the XRD method of direct measurement of areas (or heights), and Jeong et al. (2014) applied the counting grains method in micrograph obtained by microscope. The comparison of different mineralogical analysis methods is beyond the scope of the present study.

2) No significant mineralogical differences were detected between the types of dust events: red rain, dry deposition or wet deposition.

3) The mean mineralogical compositions of the silt and coarse sand fractions of the most common soils in Granada and surrounding area (Márquez, 2012) were similar to the compositional sub-triangle of the dust samples of Granada and metropolitan areas. However, the mineralogical composition of soil clay fraction was close to the apex Phyllosilicates+Iron forms. These results point to regional soils as one of possible sources of atmospheric dust collected in our samples.

4) The mineral compositions of silt and sand fractions of the other soils of the region (also included in the ternary plot) such as those of Sierra Nevada (Martín-García et al., 2004) or Sierra de Gádor (Delgado et al., 2003), being preferentially decarbonated, were only comparable with our dust samples in their relative proportions of Phyll-Fe/ Tectosilicates. Our samples contain higher contents of Phyllosilicatos+FeOx than the other soil samples (approx. 20% higher). The clay content in soil samples was richer in Phyllosilicates+FeOx than found in our collected samples.

Scheuvens et al. (2013) established different “fingerprints” of African dust origin, based on XRD’s mineralogical analysis. According to these authors, mineral dust detected in DAD samples studied here was originated from the Atlas mountains and the coastal region of the Western Sahara and Western Mauritania (Atlas - west coast), since IIlite/kaolinite ratio was >1.6, chlorite/kaolinite ratio was in the range 0.0-1.0, and carbonate content (calcite + dolomite) was intermediate to abundant (frequently >30 %), Table 3. Only samples JP01 and JP08 do not satisfy these criteria (Table 2). These results are in good agreement with the results obtained by air mass back trajectories analysis.

According to Scheuvens et al. (2013), the mineral dust, analyzed in the bibliography (Table 3), could have the same origin as the mineral dust studied here or it could come from Southern Algeria and Northern Mali. The presence of paragonite (sodium mica) in our samples (Table 2), a mineral species that is not found in African soil samples but that is abundant in Betic materials from Southern Spain (Martín-García et al., 1997) and the higher content of dolomite with regard to calcite in our samples (Table 3) point to the contribution of Betic materials from Southern Spain region to our collected dust samples This would be a new evidence of contributions from the south of Spain diluting the African dust and another possible reason for palygorskite not being detected. In the other Spanish dusts in the bibliography, paragonite has only been described in Sierra Filabres (Queralt et al., 1993) and some samples from Granada (Díaz-Hernández et al., 2011), coinciding (in accordance with our results) with calcite/dolomite ratios <1 (Table 3).

Furthermore, we calculated the mineralogical ratios-fingerprints of Scheuvens et al. (2013) for some Spanish soils (Entisols of Sierra Nevada, Martin-García et al., 2004, Luvisols and Cambisols of Sierra de Gádor, Delgado et al., 2003) that are possible sources of mineral dust collected in our samples (Table 3). In the case of Entisols, the mineralogical ratios presented the following mean values: Illite/kaolinite silt + clay = 11,4 (>1,6), chlorite/kaolinite clay = 0,7 (0.0-1.0) while for Luvisols and Cambisols the mean ratios values were: Illite/kaolinite< 50 μm = 37,6 (>1,6), chlorite/kaolinite< 50 μm = 0,4 (0.0-1.0). These results fit the Scheuvens et al. (2013)'s requirements for 'foothills of Atlas mountains and western coastal region' dust source. This casts doubt on our use of the ratios of Scheuvens et al. (2013) and provides further proof that our dusts could originate from Spanish soils.

The presence of smectite and "mixed-layer" in our samples (Table 2) does not indicate provenance either, since these are minerals found in both soils and atmospheric dust (amongst others, by Jeong et al., 2016). Nonetheless, the presence of smectite is of interest due to its being a constituent of iberulites (Díaz-Hernández and Párraga, 2008).

3.4 Rare Earth Elements (REE)

Table S1 shows the contents of rare earth elements in dust samples collected at Granada during summer 2010. Chondrite-normalized profiles (Fig. 3) present values greater than 1 (higher quantities than in the reference meteorite) and confirm the enrichment in LREE, shown by a steep negative slope (with increasing atomic number) which becomes less pronounced after Eu and almost flat in the HREE region, although some samples show an upward slope between Tm and Lu. This result is in good agreement with the values of the ratios $MREE_N/LREE_N$, between 0.09 and 0.13, and $HREE_N/LREE_N$, between 0.15 and 0.21 (Table 4).

In addition, all our samples show a pronounced negative europium anomaly (Fig. 3), with values of Eu/Eu* between 0.66 and 0.82 (Table 4). The highest Ce/Ce* anomaly value (1.17) was obtained in JP07 sample while the highest Y/Y* anomaly values (1.20 and 1.21) were observed in JP03 and JP08 samples, respectively). The rest of the samples show anomalies close to unity, mainly positive.

Rare earth elements were used also as 'fingerprints' of dust provenance comparing our dusts with their potential source materials (Tables S1 and 4; Figs. 3 and 4). For comparison we used the REE values reported for the arable layer of Spanish Soils (Locutura et al., 2012) (SS), the arable layer of European Soils (Salminen et al., 2005) (ES), African Dusts (Muhs et al., 2010) (AD), resuspended soils and aeolic materials from the Sahara-Sahel corridor (Moreno et al., 2006) (SSH), and regional materials derived from metasedimentary rocks (Sierra Nevada) (Torres-Ruiz et al., 2003) and igneous rocks (Los Pedroches batolit) (Pascual et al., 2008).

As can be seen in Table S1, the lanthanides of SS, ES, AD and SSH follow the same pattern as that of our dust samples, namely ΣLREE>ΣMREE>ΣHREE. Chondrite normalization (Fig. 3) showed enrichments in LREE with steep slopes near the HREE region, finishing with an almost flat profile in HREE region for the SS and ES soil samples and a sawtooth profile for SSH samples. However, in SSH samples, materials HM1, HM2, MON and WS3 stood out for the upward slope in the last part of the HREE region (Lu higher than its adjacent Yb), as occurred in some of our atmospheric dusts.

The mean content of ΣREE in our dust samples (70.1 ppm, Table S1) was lower than that of the upper horizons of the SS (187.6 ppm), ES, AD and SSH samples. The lower ΣREE content in our dust samples may be due to their granulometry (mainly fine sand - >50 µm, <250 µm-; Table 1, Fig. 2), coarser than SS, ES and SSH, since the REE are usually concentrated in the fine silt fractions (2 to 50 µm) and clay fractions (<2 µm) (Prudêncio et al., 1993; Aide and Smith-Aide, 2003; Marques et al., 2011).

The geochemical index $HREE_N/LREE_N$ of our dust samples (in the range 0.09 – 0.13; Table 4) is more similar to the reported for SS samples (0.10) and fairly close to the reported for ES and WS1 samples (both 0.17). MREEN/LREEN reported for SS (0.17), HM1 (Hoggar Massif) (0.19) and WS3 (Western Sahara) (0.18) are within the range of values obtained for our dust samples (0.15 – 0.21).

The geochemical anomaly of cerium (Table 4), which is not significant in most of our dust samples (close to 1.00), is similar to that reported for SS and ES samples (both 1.01), and to that of the samples CB1 (Chad) (1.02) and WS2 (Western Sahara) (1.01). In some samples, the cerium anomaly is more pronounced, e.g. in sample JP07 (1.17) and in MON (Niger) of SSH (1.11). The Eu/Eu* anomaly is always negative (<1) in all samples and the yttrium anomaly of our samples is almost similar to that reported for SS (0.98) and HM2 (Hoggar Massif) (0.94).

Consequently, in view of these findings, one cannot discard the contribution of materials from the arable layer of Spanish or European soils or from those of the Sahara Sahel and African Dust to our collected dust samples. This influence is displayed graphically, based on different geochemical indices (Fig. 4). The points representing the composition of our atmospheric dust from Granada are located in a compact group. In diagram La_N/Yb_N *vs* Eu/Eu* (Fig. 4a) the group is segregated from the rest of the materials, although the closest are the Spanish soils, materials CB1 and CB2 (from Chad), some samples of the dust from Africa described by Muhs et al. (2010) and the igneous rock from Los Pedroches (Pascual et al., 2008). In diagram Gd_N/Yb_N *vs* Eu/Eu* (Fig. 4c) the area occupied by the group of atmospheric dust from Granada is next to a sample from the Chad basin and close to the atmospheric dust from Africa, the Spanish soils, a sample from the western Sahara and, again, to the igneous rocks. In diagram La_N/Yb_N *vs* Sm_N/Yb_N (Fig. 4c) area occupied by the group of dust samples from Granada includes the representative point of Spanish soil.

3.5 Electronic micromorphology and EDX analysis of iberulites

The SEM-EDX and VPSEM-EDX results of the morphology, internal microstructure and chemistry of iberulites detected in samples collected in Granada in summer 2010 are shown in Figs. 5 and 6. The characteristics described in Figs. 5 and 6 are may be related to the formation of Iberulites. Iberulite morphology is due, amongst other processes, to the interaction of waterdrops and dust particles and their subsequent evaporation during its atmospheric transport (Fiol et al., 2001; Díaz-Hernández and Párraga, 2008) which gives rise to their pseudospherical shape and their different zones (Figs. 5a and 5c): 1) core zone, internal zone, with coarser particles; and 2) rim with finer particles and vortex, an orifice at one of the poles. This morphology determines their behaviour in the air and in the ground surface after their deposition, which may have environmental and public health implications. The porous internal structure of the iberulites (Figs. 5c and 5i) makes them relatively well-equipped to stay longer in the air compared to particles with the same volume but of much greater weight. Furthermore, their external covering by clay, in laminar clusters (Fig. 5f), gives them a certain resistance to disaggregation within the clouds, the wind and the impact with the ground and enables them to travel long distances.

When iberulites fall on a surface (ground, vegetation, roofs, paved areas) their microstructure again has an important role, since, despite the protective external covering of the rind, they can break easily, as most of their volume consists of an internal aggregate of particles with little cohesion between them, thus affording little resistance (Fig. 5i). But as we will see in the following section, the exudates bacterial make the cements sticky between mineral particles in iberulites which increase their resistance to disaggregation (Fig. 7e).

Thus, iberulites act as stores and diffusers of particles of all sizes representing a significant volume of the event. The data of Jeong et al. (2014) can illustrate this fact since giant aggregates of particles (>10 microns) from the Gobi Desert, sampled during a storm in 2012, accounted for only 20% of the total number of particles of the event as opposed to 89% of the total particles by volume.

These smaller constituent particles of iberulites, which are transported in great quantities by them and released from the iberulites during their disaggregation, can potentially be inhaled by people (as many of these particles have diameter less than 10 microns, Figs. 5 and 6) with concomitant effects on health (Párraga et al., 2013; Oduber et al., 2019). On the other hand, when these particles transported by the iberulites spread out after their impact with the ground surface they can affect the biogeochemical cycles of both land and sea (as reported by Jeong et al., 2016), modifying their chemistry by contributing materials different to those of the location.

The EDX microanalysis with SEM (Figs. 5e, 5g) of the iberulite surface (without sectioning) provided information on chemical and mineral composition. The principal constituents detected were: O, Si, Al, Ca, Fe, K, Mg, Na, Ti and S. This elemental composition is substantiated by the XRD mineralogy (Section 3.3), as we described tectosilicates (quartz and feldspars) and phyllosilicates (micas, kaolinite, smectites, mixed phases and chlorite) which contain O, Si, Al, K, Fe, K, Mg, Na, Ti; calcium and calcium magnesium carbonates (calcite and dolomite): O, Ca, Mg; iron oxides (hematite and goethite): O, Fe; and sulphates (gypsum): Ca, S.

New compositional results were obtained by mapping chemical elements and mineral compositions with VPSEM-EDX (Fig. 6). The map of Ca (Fig. 6b) detected the particles containing significant amounts of this element, belonging to calcite (40% Ca in theoretical formula: $CaCO_3$) and dolomite (21.7% Ca in $CaMg(CO_3)_2$). The points ("calcium spots") are distributed randomly and are typically located in the core of the iberulite (Figs. 6b, 6c, 6d). However, some calcium spots may be from the gypsum grains (29.4% Ca in $CaSO_4{\cdot}2H_2O$) present on the surface of the rind (Fig. 5g). The Fe map (Fig. 6e) shows the particles with relatively high Fe contents, belonging to the iron oxides present: hematite (70% Fe in Fe_2O_3) and goethite (63% Fe in FeOOH). Fe is spread throughout the inside of the iberulite in particles of various sizes. The S map (Fig. 6f), at the sensitivity used to capture the signal of this element, shows an evident ring, around 5 μm thick, which perfectly delineates the shape of the iberulite, although a few signal maxima are also observed inside iberulite. This S must be from other sources than gypsum, which is only present at <1% (Table 2).

The maps of albite ($NaAlSi_3O_8$), potassium feldspar ($KAlSi_3O_8$) and quartz (SiO_2) (Figs. 6g, 6h, 6i) show that these components are spread throughout the core of the iberulite. Another component, denoted as clay (Fig. 6j), corresponds to an elemental composition of 59.5% O, 22.9% Si, 10.3% Al, 2.2% Fe, 1.4% Mg, 1.2% K and 0.2% Ti. These are phyllosilicate phases which are abundant in our dust samples (Table 2): illite, smectite, mixed layers, paragonite or chlorite. Clay minerals define the spherical morphology (circular in 2D) of the iberulite, which help to fill it from the inside outwards and clearly dominate the exterior zone ("rind").

These findings highlighting the spatial distribution of the component elements and minerals (Fig. 6), graphically and concisely, go further than previous studies (Díaz Hernández and Párraga, 2008; Cuadros et al., 2015) and provide more evidence for the hypotheses on the formation of iberulites. The chemical elements Ca and Fe, and the mineral phase particles calcite, dolomite, iron oxides, quartz, albite and potassium feldspar (Fig. 6) are distributed within the core of the iberulite. On the other hand, the “clay minerals” (Fig. 6j) do explain the nature of the iberulite and its spherical shape as they constitute both the greater part of the particle grouping in its interior and the mass of its rind. If the quantity of clay is estimated from the area occupied in Fig. 6 it would be around 50%, close to phyllosilicates content in the dust (around 40% in most cases) measured by XRD (Table 2).

Another components involved in defining the morphology of the iberulite are sulphur phases, S, which mark out a ring and act as a covering or casing (Fig. 6f). However, the S must be from a different source than the gypsum as its content is less than 1% (Table 2), although gypsum was detected on the surface of the rind (Fig. 5g). We believe, firstly, that S from Fig. 6f are elemental sulphur particles (100% S), supported by the noticeable shine of some of the particles in the rim of Fig. 6, and, secondly this is sulphur that has been incorporated into the expandable 2:1 phyllosilicates. In any case, the S in the iberulites seems to originate from the atmospheric processing.

Several studies (Kulshrestha et al. 2003; Korhonen et al. 2003; Díaz-Hernández and Párraga 2008) have revealed that mineral dust particles get often coated with sulphate (and other soluble material) by SO2 oxidation to SO4 during in cloud scavenging by heterogeneous nucleation.

In our case, the H2SO4 could have two origins: a) condensation of gaseous sulfuric acid on iberulite rind; b) absorption of atmospheric SO2 into liquid water droplets and dust particles in clouds and on nanoclays clusters in the rind of iberulite (see Figure 8, point 5; Figure 6f). The high surface to volume ratio that clay minerals have together with the influence of the liquid-solid interface, allows nucleation proceeds via direct vapor deposition onto the high surface of nanoclays clusters.

Rodriguez et al (2011) attribute to industrial emissions in North Africa (Morocco, Algeria, Tunisia and Libya) that the major sources of SOx are emissions from crude oil refineries and power plants. Lastly, the intense ship traffic in Mediterranean Sea means that shipping emissions are currently increasing. Impacts from shipping emissions on SO2 atmospheric concentrations were reported over European sea areas (Russo et al. 2018).

3.6 Characteristics of biological activity of iberulites and its importance on their formation

SEM and HRTEM images of the iberulites shown in Figs. 5 and 7 reveal the presence of many biological species in iberulites, including strands of vegetable matter which act as nucleating agents of the dust particles for later formation of the iberulite (Fig. 5d). We also found remains of centric diatoms, of around 20 µm, probably of the Family *Aulacoseiraceae* (Class: *Coscinodiscophyceae*, Order: *Aulacoseirales*), Fig. 5g. The most abundant microorganism associated with African dust intrusion over Granada in 2010 were *Proteobacteria* (74% of the total) and *Firmicutes* (19% of the total), with minor presence of *Bacteriodites* and *Actiniobacteria* (<1% of the total) (Figs. 5h, 7c, 7d, 7e) (Sánchez de la Campa et al. 2013). We even found brochosomes (Fig. 5f), superhydrophobic protein-secreting particles with diameter in the range 0.2-20 µm produced by the Malphigian tubules of grasshoppers (Cicadellidae), one of the most diverse and abundant families of insects (Rakitov and Gorb, 2013). The presence of biological remains in iberulites has already been detected by Fiol et al. (2005), Díaz-Hernández et al. (2012) and Párraga et al. (2013), even though they were not reported to participate in the iberulite genesis.

As shown in Fig. 5h, bacteria tend to appear in colonies clustered together in microsites, which are often situated in micro-depressions on the surface of the iberulite. However, they are sometimes found within the matrix (Fig. 7d). A striking feature, never observed before, is the grouping together of bacterial bodies with mineral grains by means of extremely fine filaments (Fig. 7f) and even biofilms (Fig. 7e). These filaments/biofilms could be flagellae, pili, extracellular polymeric substances (EPS, biofilms) or exudates produced by the bacteria. They are preferentially observed on the iberulite surface, being involved in the formation of microbial aggregates adhered to mineral surfaces. The results indicate that the bacteria might contribute to the protection and stability of the iberulite, reinforcing it and contributing to its internal configuration. Thus, bacteria act as aggregation agent.

These new observations and results have led us to take into account the role of bacteria in iberulite genesis and to reconsider the previous hypothesis regarding the iberulite genesis proposed by Díaz-Hernández and Párraga (2008) and Cuadros et al. (2015). The new proposed iberulite genesis scheme is described in detail in Fig. 8. Mineral particles (and possibly soil organic matter) and their associated bacteria (Fig. 7a) are incorporated from soils without vegetation cover into the atmosphere by wind action (Fig. 8-1 and 8-2). The atmospheric dust (mineral, bacteria and soil organic matter) from the surface (Fig. 8-2) could fall again to surface by dry deposition (Fig. 8-3) or be involved in the cloud formation processes (Fig. 8-5). In the former mechanism the dust aerosol particles (microbes, mineral and other particles) act as cloud condensation nuclei or collides with pre-existing water droplets within the cloud (Fig. 8-5) leading to the formation of small droplets which increase in size through coalescence to become collector drops (Fig. 8-6). Attaining a critical radius these collector drops leave the cloud, becoming larger "falling droplets" (Fig. 8-7) which, through gravity, interact with the atmospheric dust column, with an increase in radius and velocity (and therefore in Reynolds number) and abandon the cloud, once again collecting mineral particles and microorganisms (bacteria, virus, nanoplankton, diatoms, etc.) and finally becoming mature iberulites (with size between 34 and 111 µm). As these iberulites are extremely porous with low density (bulk density 0.65 g cm^{-3} and porosity about 50%) (Díaz-Hernández and Párraga, 2008) they can spend longer time in the atmosphere than mineral particles of similar size. Moisture is present throughout this process due to the iberulites being composed of abundant hygroscopic clay minerals with high water retention (Fig. 6j) and originating from drops of water. Consequently, bacterial growth and their production of exudates (EPS) such as biofilm or filaments (Fig. 7e) is facilitated. These bacteria and their products are either incorporated into the mass of the iberulite (Fig. 7d) or remain on the surface (Fig. 7e, 7f) and thus contribute to the formation and stabilization of the iberulite as a body and compensate its fragility.

Many of these bacteria are viable and resistant to the exposition to the ultraviolet radiation because they are carried within the clayey matrix of iberulite (Fig. 7d) and can survive for a long time in the hostile atmosphere (Yamaguchi et al., 2012; Favet et al., 2013; Sanchez de la Campa et al., 2013).

In Fig. 7d (ultra-thin section of iberulite), we have detected nanoparticles containing EDX spectrum iron (less than 100 nm) inside the bacteria, in the cell wall and outside, that can induce bacterial growth and biofilm formation (Borcherding et al., 2014).

In Figs. 7e and 7f we have appreciates exudates of EPS and a filament of bacterial origin, confirming that there is microbial activity within the structure of iberulite.

This biological material can thus travel through the atmosphere, even between continents because the dust and iberulites can be transported from the Sahara-Sahel within the Saharan Air Layer (SAL) which rises to about 500 mb (altitude around 6 km) to South America (Amazonia), the North Atlantic-Caribbean area and Europe (Díaz-Hernández and Párraga, 2008).

This marks the end of the cycle of iberulite formation which started with the deflation of bacteria and soil particles from the ground and ended with the growth of these bacteria inside the iberulite and their return to the ground surface (Fig. 8).

4. Conclusions

The paper show that the dust samples collected in Granada in 2010 (14 samples) are mineralogically heterogeneous, both qualitatively and quantitatively, such that a single sample is not sufficient for determination the origin of the sampled particles. The mineralogical composition analysis showed that the sampled particles were originated from the north-northwest of Africa (Atlas – west Sahara – Mauritania) and local/regional soil sources. The use of REE as fingerprints does not rule out the contribution of diverse materials such as African aeolian dusts or Spanish soils to our dusts.

The phenomena of particle aggregation are frequent in the atmosphere with no patterns of structural organization. The complex shapes of these polymineral aggregates are irregular. All of these shapes are different from iberulites, a new type of quasi-spherical giant atmospheric particle formed under special conditions in periods corresponding to higher levels of dust deposition. A distinct feature of iberulites is the vortex, which is related with their formation mechanism and the distribution of mineral grains.

Thus, we can redefine an iberulite (bioaerosol) as "a microspherulite of clayey mud, mechanically generated and formed in the troposphere by complex mineral grains-bacteria-water-gas interactions. It is a coassociation with axial geometry, made up of well-defined mineral grains, together with biological constituents, bacterial and non-crystalline compounds (extracelular polymeric substances, EPS) structured on a coarse-grained core internal (with sizes less than 10 microns) and a relatively more sulphurated pinkish clayey ring (nano-clays in laminar clusters) with only a typical vortex at one of the poles and an average size of 100µm. "

Iberulites were present in all dust samples analyzed in this study with mass fraction between 0.7 and 9.2%. The SEM-microstructure analysis also shows that the clay and the S components are decisive in determining its spherical shape. On the other hand, the chemical elements Ca and Fe and the mineral phase particles (calcite, dolomite, iron oxides, quartz, albite and potassium feldspar) are distributed in the mass of the iberulite without relevance for its spherical configuration. The micro-morphological analysis evidences the role of bacteria in iberulite formation, which, through bacterial growth in the clouds and the descent to earth, together with the production of EPS conjunct the mineral particles and stabilize the pseudospheres externally. Bacterial can be an important agent in aggregation, which has not been found or considered previously in the formation of iberulite. It is a new viewpoint. With these new observations and results have led us to take into account the role of bacteria in iberulite formation and to reconsider the previous hypothesis regarding the iberulite formation proposed by previous works.

Finally, iberulites can be shuttles for the intercontinental transport of microorganisms, which can grow inside it, being protected from UV radiation and having an environment rich in nutrients. The iberulites are the tangible evidence of the fluid-dynamic theory applied to the interaction of water drops, gases and dust particles in the atmosphere, giving rise to shapes with a vortex, that until now, they had been explained in laboratory studies.

Acknowledgments

This work was supported by the Spanish Agencia Estatal de Investigación (AEI) through projects CGL2016-80308-P, CGL2016-81092-R and CGL2017-90884-REDT, and by the European Union's Horizon 2020 research and innovation program through project ACTRIS-2 (grant agreement No 654109). Also, we are thankful to EMEP (European Monitoring and Evaluation Programme) for providing the air quality data from background station.

5. References

Aide, M., Smith-Aide, C., 2003. Assessing soil genesis by rare-earth elemental analysis. Soil Sci. Soc. Am. J. 67, 1470-1476.

Ávila, A., Queralt-Mitjans, I., Alarcón, M., 1997. Mineralogical composition of African dust delivered by red rains over northeastern Spain. J. Geophys. Res. Atmos. 102(D18), 21977-21996.

Barahona, E., 1974. Arcilla de ladrillería de la provincial de Granada. Evaluación de algunos ensayos de materias primas. Tesis Doctoral. Univ. Granada. 398p.

Bergametti, G., Foret, G., 2014. Dust deposition. In Mineral dust: a Key Player in the Earth System (eds. P. Knippertz and J.-B.W. Stuut) Springer, Dordrecht, pp.179-200.

Borcherding, J., Baltrusaitis, J., Chen, H., Stebounova, L., Wu, C. M., Rubasinghege, G., Comellas, A. P. (2014). Iron oxide nanoparticles induce Pseudomonas aeruginosa growth, induce biofilm formation, and inhibit antimicrobial peptide function. Environ. Sci. Nano, 1(2), 123-132.

British Geological Survey (BGS), 2011. “Rare Earth Elements” (BSG, 2011; https://www.bgs.ac.uk/downloads/start.cfm?id=1638).

Calero, J., Delgado, R., Delgado, G., Martín-García, J.M., 2009. SEM image analysis in the study of a soil chronosequence on fluvial terraces of the middle Guadalquivir (southern Spain). Eur. J. Soil Sci. 60, 465–480.

CALIMA. Dirección General de Calidad y Evaluación Ambiental del Ministerio de Agricultura, Alimentación y Medio Ambiente, España. Link: http://www.calima.ws/

Calvo, A.I., Olmo, F.J., Lyamani, H., Alados-Arboledas, L., Castro, A., Fernández-Raga, M., Fraile, R., 2010. Chemical composition of wet precipitation at the background EMEP station in Víznar (Granada, Spain) (2002–2006). Atmos. Res. 96(2-3), 408-420.

Cuadros J., Díaz-Hernández J.L., Sánchez-Navas, 2015. Role of clay minerals in the formation of atmospheric aggregates of Saharan dust Atmos. Environ. 120, 160-172.

De la Rosa, J., Sánchez de la Campa, A.M., Alastuey, A., Querol, X., González-Castanedo, Y., Fernández-Camacho, R., Stein, A.F., 2010. Using PM10 geochemicals maps for defining the origin of atmospheric pollution in Andalusia (Southern Spain). Atmos. Environ. 44, 4595-4605.

Delgado R., Barahona E., Huertas F., Linares J., 1982. Los Mollisoles de la Cuenca Alta del Río Dílar (Sierra Nevada). Anales de Edafología y Agrobiología. 41, 59-82.

Delgado, R., Martín-García, J.M., Oyonarte, C., Delgado, G., 2003. Genesis of the terrae rossae of the Sierra Gádor (Andalusia, Spain). Eur. J. Soil Sci. 54, 1-16.

Díaz Hernández, J.L., Párraga, J., 2008. The nature and tropospheric formation of iberulites: Pinkish mineral microspherulites. Geochim. Cosmochim. Acta. 72, 3883-3906.

Díaz-Hernández, J. L., Martín-Ramos, J. D., López-Galindo, A., 2011. Quantitative analysis of mineral phases in atmospheric dust deposited in the south-eastern Iberian Peninsula. Atmos. Environ. 45(18), 3015-3024.

Diaz-Hernandez, J. L., Sanchez-Navas A., 2016. Saharan dust outbreaks and iberulite episodes, J. Geophys. Res. Atmos. 121, 7064–7078.

Díaz-Hernández, J. L. , Sánchez-Soto, P. J., Serrano-Delgado, A., 2012. Biological nanostructures associated to iberulites: a SEM study. Curr. Microsc. Contrib. Adv. Sci. and Techn. 154-161

Directive, 2008. 50/EC of the European Parliament and the Council of 21 May 2008. Relating to ambient air quality and cleaner air for Europe. OJL 152, 11.6.2008, p.1-44.

Draxler, R. R., Rolph, G. D., 2003: HYSPLIT (HYbrid single- particle Lagrangian integrated trajectory) Model access via NOAA ARL READY Website (http://www.arl.noaa.gov/ready/hysplit4.html), NOAA Air Resources Lab., Silver Spring, MD, USA.

EMEP, 2001. EMEP manual for sampling and chemical analysis. EMEP/CCCReport 1/95, Revision 1/2001, NILU, Norge.

Engelbrecht, J.P., Moosmüller, H., Pincok, S., Jayanty, R.K.M., Lersch, T., Casuccio, G., 2016.Technical note: Mineralogical, chemical, morphological, and optical interrelationships of mineral dust re-suspensions. Atmos. Chem. Phys. 16, 10809-10830.

Favet, J., Lapanje, A., Giongo, A., Kennedy, S., Aung, Y. Y., Cattaneo, A., Schnetger, B., Davis-Richardson, A.G., T Brown C., Kort R., Brumsack HJ, Schnetger B., Chappell A., Kroijenga J., Beck A., Schwibbert K., Mohamed AH., Kirchner T., Dorr de Quadros P., W Triplett E., Broughton W.J., Gorbushina, A., 2013. Microbial hitchhikers on intercontinental dust: catching a lift in Chad. ISME J. 7(4), 850.

Fiol, L., Guijarro, J.A., Forno´s, J.J., 2001. Las lluvias de barro en el Mediterráneo Occidental: el caso de Mallorca. Rev. Climatol. 1, 7-20.

Fiol, L., Fornós, J. J., Gelabert, B., Guijarro, J. A., 2005. Dust rains in Mallorca (Western Mediterranean): Their occurrence and role in some recent geological processes. Catena. 63(1), 64-84.

Fornós, J. J., Fiol, L. A., Pastor, J.A.G., 2004. Episodis significatius de pluges de fang ocorregudes els mesos de febrer i març de 2004 a Mallorca (Mediterrània occidental). Significative dust rain on february and march of 2004 episodes in Mallorca (Western Mediterranean). Bolletí de la Societat d'Història Natural de les Balears. 47, 43-50.

Jeong, G. Y., Kim, J. Y., Seo, J., Kim, G. M., Jin, H. C., Chun, Y., 2014. Long-range transport of giant particles in Asian dust identified by physical, mineralogical, and meteorological analysis. Atmos. Chem. Phys. 14, 505-521.

Jeong, G. Y., Nousiainen, T., 2014. TEM analysis of the internal structures and mineralogy of Asian dust particles and the implications for optical modeling. Atmos. Chem. Phys. 14, 6619-6661.

Jeong G. Y., Achterberg, E. P., 2014. Chemical and mineralogy of clay minerals in Asian and Saharan dust and the implications for iron supply to the oceans. Atmos. Chem. Phys. 14, 12415-12428.

Jeong, G. Y., Park, M. Y., Kandler, K., Nousiainen, T., Kemppinen, O., 2016. Mineralogical properties and internal structures of individual fine particles of Saharan dust. Atmos. Chem. Phys. 16(19), 12397-12410.

Korhonen, H., Napari, I., Timmreck, C., Vehkamäki, H., Pirjola, L., Lehtinen, K. E. J., Lauri, A., Kulmala, M. (2003). Heterogeneous nucleation as a potential sulphate-coating mechanism of atmospheric mineral dust particles and implications of coated dust on new particle formation. J. Geophys. Res. 108(D17).

Korotev, R.L., 2009. “Rare earth plots” and the concentrations of rare earth elements (REE) in chondritic meteorites. Web site: http://meteorites.wustl.edu/goodstuff/ree-chon.htm.

Kulshrestha, M. J., Kulshrestha, U. C., Parashar, D. C., Vairamani, M. (2003). Estimation of SO4 contribution by dry deposition of SO2 onto the dust particles in India. Atmos. Environ. 37(22), 3057-3063.

Kuo, J., 2007. Electron Microscopy. Methods and Protocols, second ed. Humana Press, Inc. Totowa, New Jersey.

Kuzmichev, A.A., Azarov, V.N., Kuzmichev A.V., 2017. The research of contamination regularities of historical buildings and architectural monuments by methods of computer modeling. MATEC. Web of conferences. 129, 05002.

Laveuf, C., Cornu, S., 2009. A review on the potentiality of Rare Earth Elements to trace pedogenetic processes. Geoderma. 154, 1-12.

Locutura, J., Bel-lan, A., García, C.A., Martínez, S., 2012. Atlas Geoquímico de España. Madrid: Instituto Geológico y Minero de España.

Lyamani, H., Olmo, F.J., Alados-Arboledas, L., 2005. Saharan dust outbreak over southeastern Spain as detected by sun photometer Atmos. Environ. 39(38), 7276-7284.

Lyamani, H., Olmo, F.J., Alados-Arboledas, L., 2010. Physical and optical properties of aerosols over an urban location in Spain: seasonal and diurnal variability. Atmos. Chem. Phys., 10, 239-254.

Marques, R., Prudencio, M.I., Dias, M.I., Rocha, F., 2011. Patterns of rare earth and other trace elements in different size fractions of clays of Campanian–Maastrichtian deposits from the Portuguese western margin (Aveiro and Taveiro Formations). Chem Erde-Geochem. 71, 337-347.

Márquez Crespo, R., 2012. El cuarzo de la fracción arena fina en suelos de la provincia de Granada. Universidad de Granada.

Martin, J. D., 2004. XPowder A software package for Powder X-Ray diffraction analysis, Granada, Spain. ISBN 978-84-16478-87-3.

Martín-García, J.M., Delgado, G., Sánchez-Marañón, M., Párraga, J.F., Delgado, R., 1997. Nature of dioctahedral micas in Spanish red soils. Clays Clay Miner. 32, 107–121.

Martín-García, J.M., Aranda, V., Gámiz, E., Bech, J., Delgado, R., 2004. Are Mediterranean mountains Entisols weakly developed? The case of Orthents from Sierra Nevada (Southern Spain). Geoderma. 118, 115-131.

McDonough, W.F., Sun, S., 1995. The composition of the Earth. Chem. Geol. 120, 223–253.

Moreno, T., Querol, X., Castillo, S., Alastuey, A., Cuevas, E., Herrmann, L., Mounkaila, M., Elvira, J., Gibbons, W., 2006. Geochemical variations in aeolian mineral particles from the Sahara-Sahel Dust Corridor. Chemosphere. 65, 261-270.

Mourier, B., Poulenard, J., Chavel, C., Faivre, P., Carcaullet, C., 2008. Distinguishing subalpine soil types using extractable Al and Fe extractions and REE geochemistry. Geoderma. 145, 107-120.

Muhs, D. R., Budahn, J., Skipp, G., Prospero, J. M., Patterson, D., Bettis III, E. A., 2010. Geochemical and mineralogical evidence for Sahara and Sahel dust additions to Quaternary soils on Lanzarote, eastern Canary Islands, Spain. Terra Nova, 22(6), 399-410.

Oduber, F., Calvo, A.I., Blanco-Alegre, C., Castro, A., Nunes, T., Alves, C., Sorribas, M., Fernández-González, D., Vega-Maray, A.M., Valencia-Barrera, R.M., Lucarelli, F., Calzolai, G., Alonso-Blanco, E., Fraile, B., Fialho, P., Coz, E., Prevot, A.S.H., Pont, V., Fraile, R., 2019. Unusual winter Saharan dust intrusions at Northwest Spain: Air quality, radiative and health impacts. Sci. Total Environ. 669, 213-228.

Párraga, J., Delgado, G., Martín-García, J.M., Olmo, F.J., Delgado, R., 2013. Iberulitos: partículas atmosféricas “gigantes” potencialmente inhalables. Actualidad Médica. 98, 86-91.

Pascual, E., Donaire, T., Pin, C., 2008. The significance of microgranular enclaves in assessing the magmatic evolution of a high-level composite batholith: A case on the Los Pedroches Batholith, Iberian Massif, Spain. Geochem. J. 42, 177-198.

Pey, J., Querol, X., Alastuey, A., Forastiere, F., Stafoggia, M., 2013. African dust outbreaks over the Mediterranean Basin during 2001–2011: PM10 concentrations, phenomenology and trends, and its relation with synoptic and mesoscale meteorology. Atmos. Chem. Phys. 13, 1395-1410.

Posfai, M., Axisa, D., Tompa, E., Freney, E., Bruintjes, R., Buseck P., 2013. Interactions of mineral dust with pollution and clouds: An individual-particle TEM study of atmospheric aerosol from Saudi-Arabia. Atmos. Res. 122, 347-361.

Prudêncio, M.I., Braga, M.A.S., Gouveia, M.A., 1993. REE mobilization, fractionation and precipitation during weathering of basalts. Chem. Geol. 107, 251–254.

Queralt-Mitjans, I., Domingo, F., Sole-Benet, A., 1993. The influence of local sources on the mineral content of bulk deposition over an altitudinal gradient in the Filabres Range (SE Spain). J. Geophys. Res. Atmos. 98(D9), 16761-16768.

Rakitov, R., & Gorb, S. N. (2013). Brochosomal coats turn leafhopper (Insecta, Hemiptera, Cicadellidae) integument to superhydrophobic state. Proceedings of the Royal Society B: Biological Sciences, 280(1752), 20122391.

Reyes, M., Díaz, J., Tobias, A., Montero, J.C., Linares, C., 2014. Impact of Saharan dust particles on hospital admissions in Madrid (Spain). Int. J. Environ. Health. Res. 24(1), 63-72.

Rodriguez, S., Querol, X., Alastuey, A., Kallos, G., Kakaliagou, O., 2001. Saharan dust contributions to PM10 and TSP levels in Southern and Eastern Spain. Atmos. Environ. 35, 2433-2447.

Rodríguez González, S., Alastuey, A., Alonso-Pérez, S., Querol, X., Cuevas Agulló, E., Abreu Afonso, J., Viana, M., Pandolfi, M., de la Rosa, J. (2011). Transport of desert dust mixed with North African industrial pollutants in the subtropical Saharan Air Layer. Atmos. Chem. Phys. Discuss. 11, 8841-8892.

Rodriguez-Navarro, C., Di Lorenzo, F., Elert, K., 2018. Mineralogy and physicochemical features of Saharan dust wet deposited in the Iberian Peninsula during an extreme red rain event. Atmos. Chem. Phys. 18(13), 10089–10122.

Rollinson, H.R., 1993. Using Geochemical Data: Evaluation, Presentation, Interpretation. Harlow: Prentice Hall.

Russo, M. A., Leitão, J., Gama, C., Ferreira, J., Monteiro, A. (2018). Shipping emissions over Europe: a state-of-the-art and comparative analysis. Atmos. Environ. 177, 187-194.

Salminen, R. (Chief-editor), Batista, M. J., Bidovec, M., Demetriades, A., De Vivo, B., De Vos, W., Duris, M., Gilucis, A., Gregorauskiene, V., Halamic, J., Heitzmann, P., Lima, A., Jordan, G., Klaver, G., Klein, P., Lis, J., Locutura, J., Marsina, K., Mazreku, A., O'Connor, P. J., Olsson, S.Å., Ottesen, R.-T., Petersell, V., Plant, J.A., Reeder, S., Salpeteur, I., Sandström, H., Siewers, U., Steenfelt, A., Tarvainen, T., 2005. Geochemical Atlas of Europe. Part 1: Background Information, Methodology and Maps. Espoo, Geological Survey of Finland. Available at: http://weppi.gtk.fi/publ/foregsatlas/index.php

Sánchez de la Campa, A. M., García Salamanca, A., Solano, J., De la Rosa, J., Ramos, J.L., 2013. Chemical and microbiological characterization of atmospheric particulate matter during an intense african dust even in southern Spain. Environ. Sci. Technol. 47(8), 36360-3638.

Scheuvens, D., Schütz, L., Kandler, K., Ebert, M., Weinbruch, S., 2013. Bulk composition of northern African dust and its source sediments. A compilation. Earth. Sci. Rev. 116, 170-194.

Schultz L.G. (1964) Quantitative interpretation of mineralogical composition from X-ray and chemical data for the Pierre Shale. US Geol. Surv. Prof Pap., 391 C., 31 pp.

Torres-Ruiz, J., Pesquera, A., Gil-Crespo, P.P., Velilla, N., 2003. Origin and petrogenetic implication of turmaline-rich rocks in the Sierra Nevada (Betic Cordillera, southeastern Spain). Chem. Geol. 197, 55-86.

Vahlsing, C., Smith, K. R., 2012. Global review of national ambient air quality standards for PM10 and SO_2 (24 h). Air Qual. Atmos. Health. 5(4), 393-399.

Valenzuela, A., Olmo, F.J., Lyamani, H., Antón, M., Quirantes, A., Alados-Arboledas, L., 2012a. Analysis of the columnar radiative properties retrieved during African desert dust events over Granada (2005–2010) using principal plane sky radiances and spheroids retrieval procedure. Atmos. Res. 104-105, 292-301.

Valenzuela, A., Olmo, F.J., Lyamani, H., Anton, M., Quirantes, A., Alados-Arboledas, L., 2012b. Classification of aerosol radiative properties during African desert dust intrusions over southeastern Spain by sector origins and cluster analysis. J. Geophys. Res. Atmos. 117. D06214 doi:10.1029/2011JD016885. 2012b.

Varga, G., Üjvári, G., Kovács, J., 2014. Spatiotemporal patterns of Saharan dust outbreaks in the Mediterranean Basin. Aeolian Res. 15, 151-160.

Wang, G., Li, J., Ravi, S., Van Pelt, R.S., Costa P.J.M., Dukes D., 2017. Tracer techniques in aeolian research: Approaches, applications, and Challenges. Earth Sci. Rev. 170, 1–16.

Yamaguchi, N., Ichijo, T., Sakotani, A., Baba, T., Nasu, M., 2012. Global dispersión of bacterial cells on Asian dust. Sci. Rep. 2, 525.

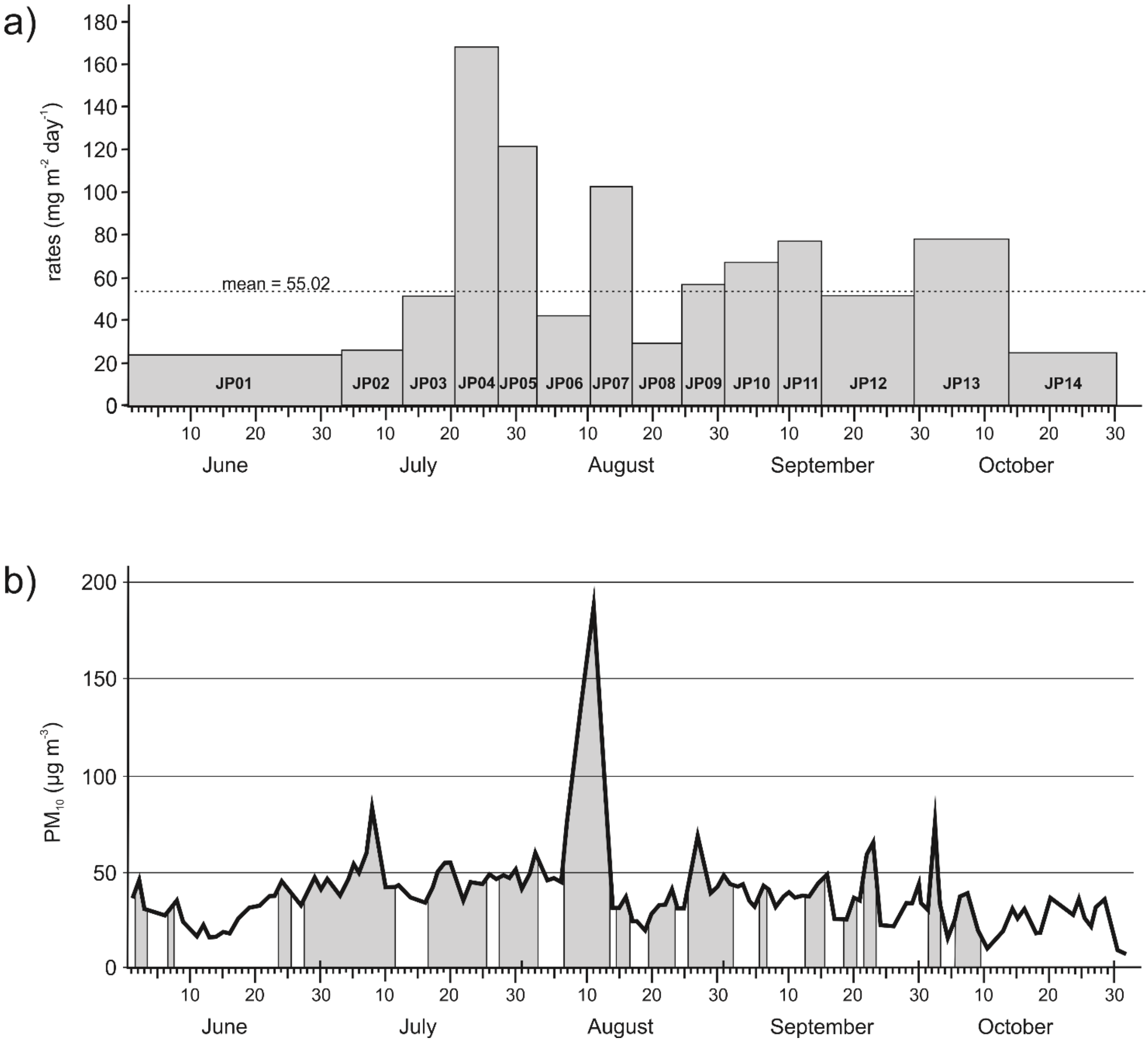

Fig. 1. a) Deposition rates (mg m^{-2} day^{-1}) of the 14 samples (JP01 to JP14) from June to October 2010. b) PM10 concentrations during summer 2010. Shaded areas show days of Saharan Dust Outbreaks according to CALIMA.

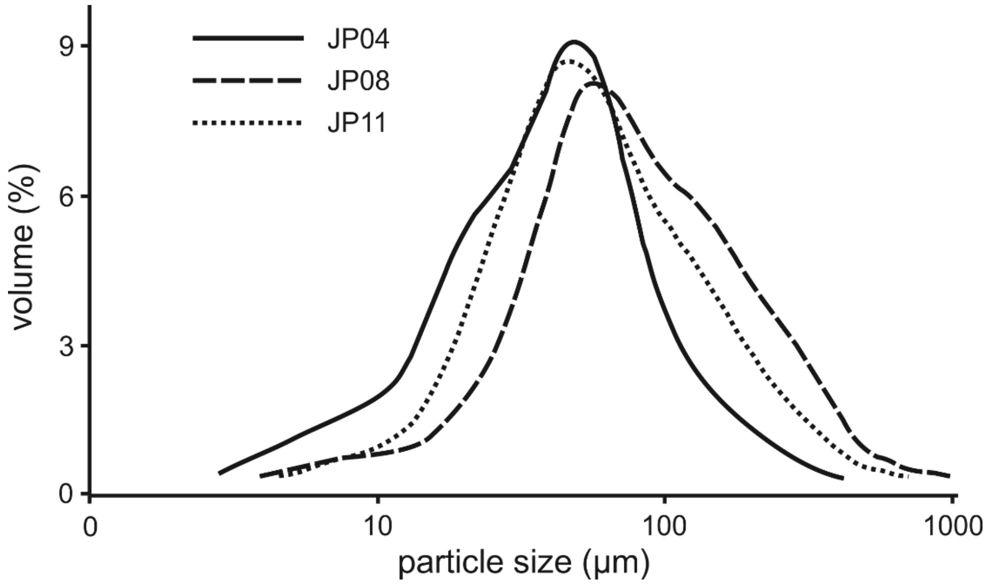

Fig. S1. Selected granulometric curves (laser diffraction).

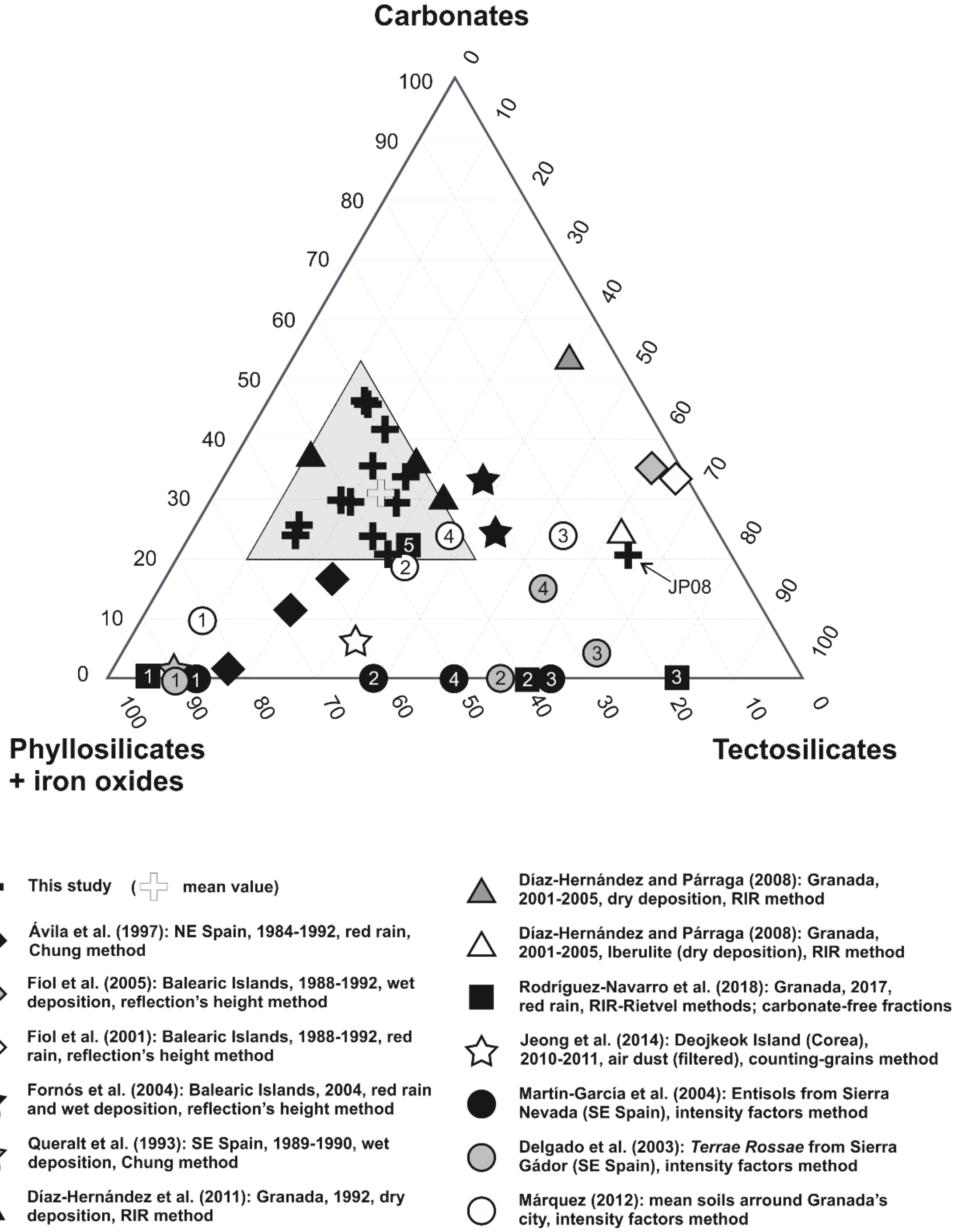

Fig. 2. Ternary plot of Phyllosilicates + iron oxides – Carbonates – Tectosilicates (% from XRD analysis) of the samples analyzed in this study and other samples of dust deposited in the Iberian Penninsula and Balearic Islands. Tectosilicates = quartz + feldspars; carbonates = calcite + dolomite. Numbers within symbols indicate granulometric fractions: 1, clay (<2 μm); 2, silt (2 – 50 μm); 3, fine sand (50 – 250 μm; 4, coarse sand (250 – 2000 μm); 5, bulk sample. The shaded triangle is for samples from Granada and metropolitan area including samples from this study (except sample JP08) and others from the bibliography.

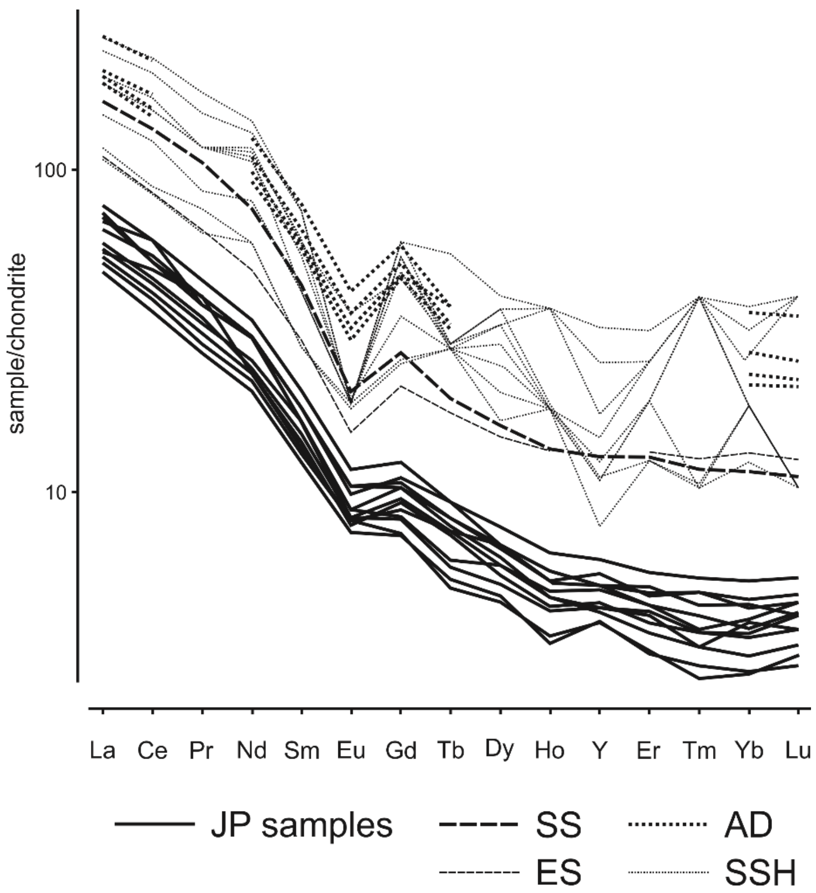

Fig. 3. Chondrite normalization of REE contents of samples of atmospheric dust and other materials. Spanish soils (SS), African dust (AD), European soils (AS), SSH (Sahara-Sahel corridor).

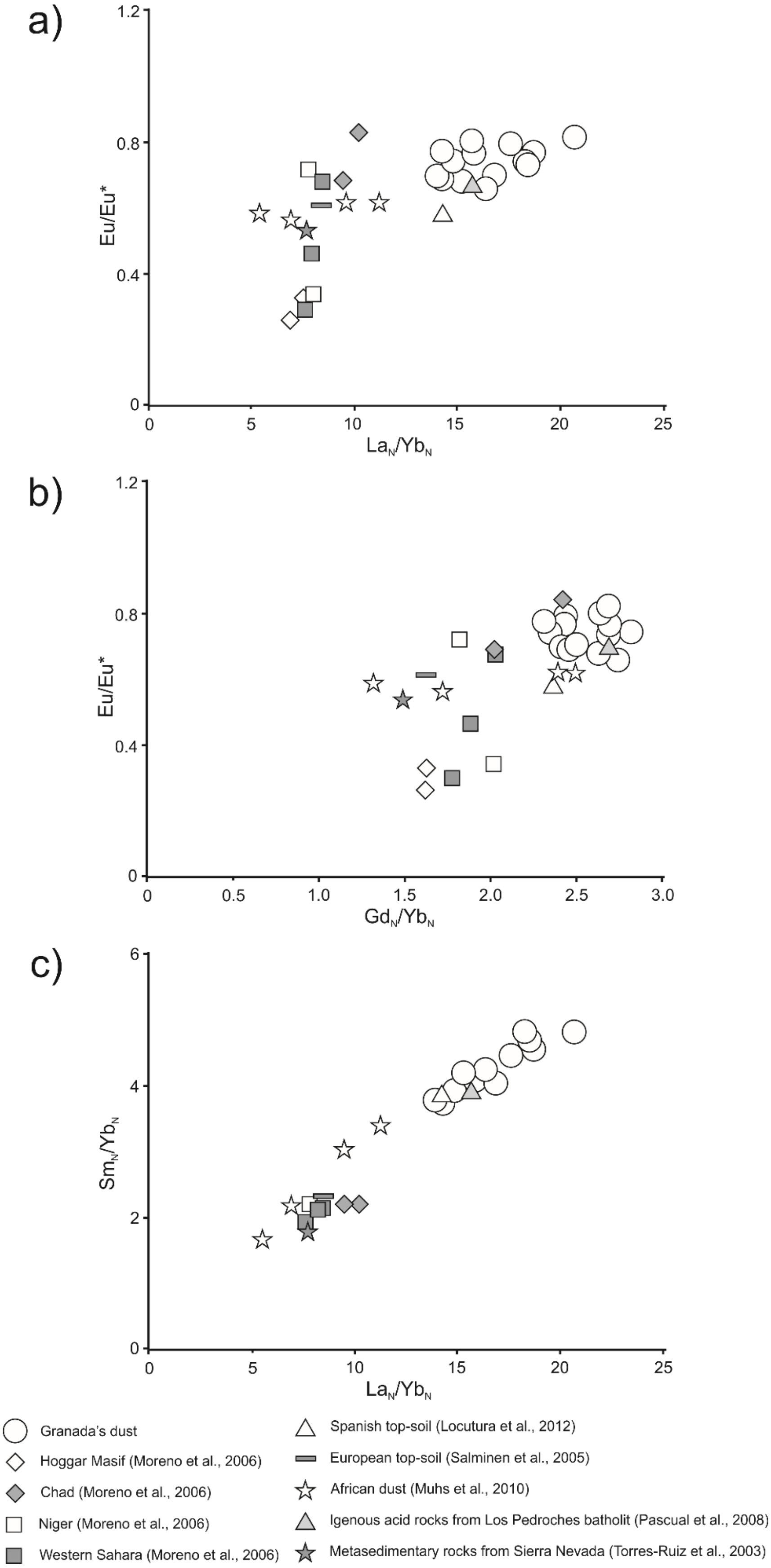

Fig. 4. Diagrams of geochemical indices in atmospheric dust (this study) and other materials. a) LaN/YbN vs. Eu/Eu*, b) GdN/YbN vs. Eu/Eu* and c) LaN/YbN vs. SmN/YbN.

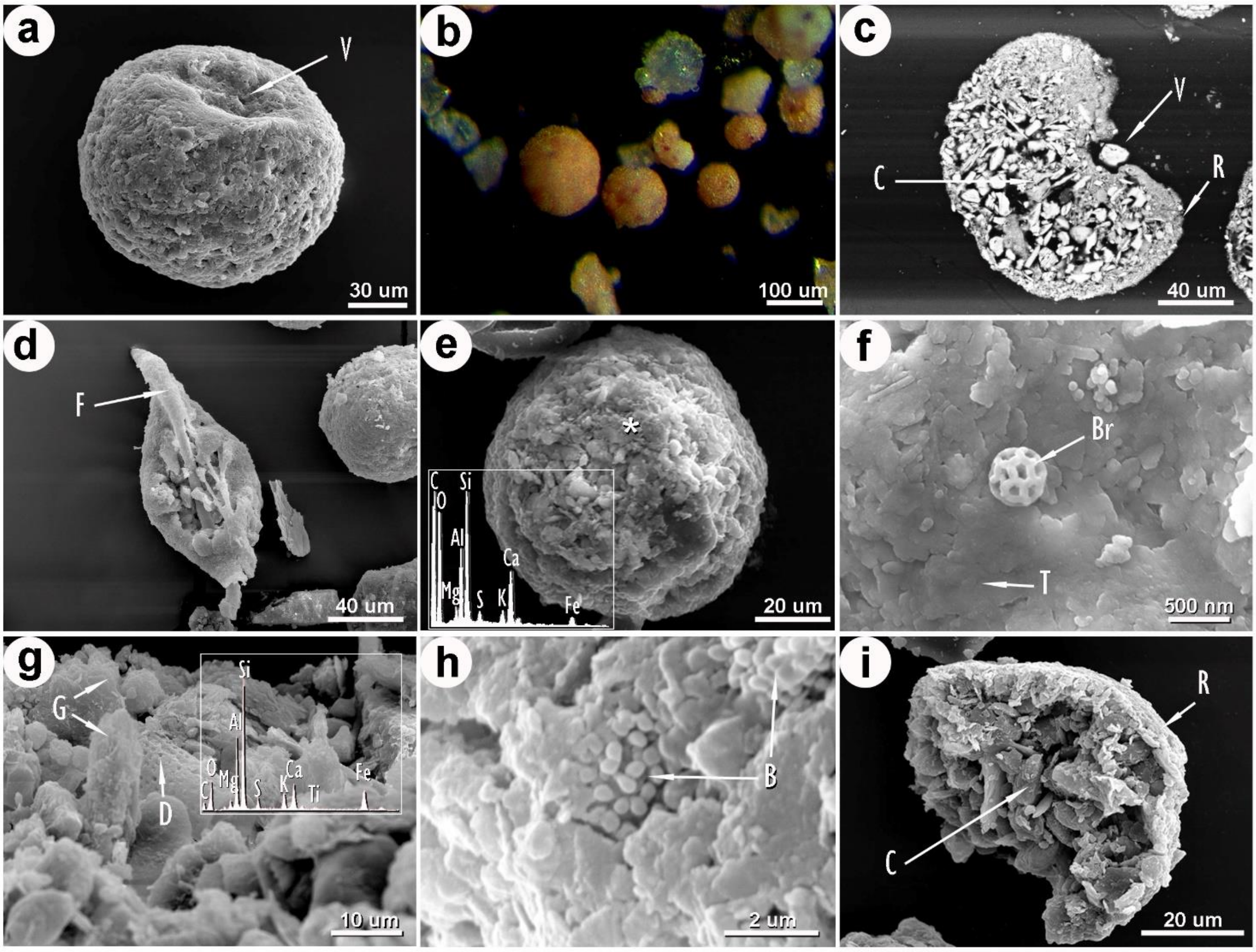

Fig. 5. SEM (conventional) and stereomicroscope photographs, and EDX spectra of iberulites (samples from deposited dust, summer 2010). These are aggregates (mainly quasi-spherical) of mineral particles, thus classified as spherulites. **a)** SEM image of the upper part of an iberulite (V = vortex). **b)** Stereomicroscopy photograph of a field of iberulites. **c**) SEM image of sectioned iberulite. (C = corex; R = rind; V = vortex) **d**) SEM image of a spindle shaped iberulite formed on a filamentous vegetable particle (F). **e)** SEM Image of spherical cap opposite the vortex with EDX microanalysis in the location marked with (*). **f)** Detail of the laminar rind surface, which can be considered as tactoids (T). Presence of a brochosome (Br). **g)** Detail of the surface of the opposite hemisphere to the vortex and microanalysis. Crystal habit of some suggests sulphate crystals, as gypsum (G). Remains of the siliceous frustule of a centric diatom (*Aulacoseiraceae*-like) (D. **h)** Surface with successive layers of clay and carbonates. Microsites with groups (colonies) of bacteria (B). **i)** Fragmented iberulite (C = core; R = rind).

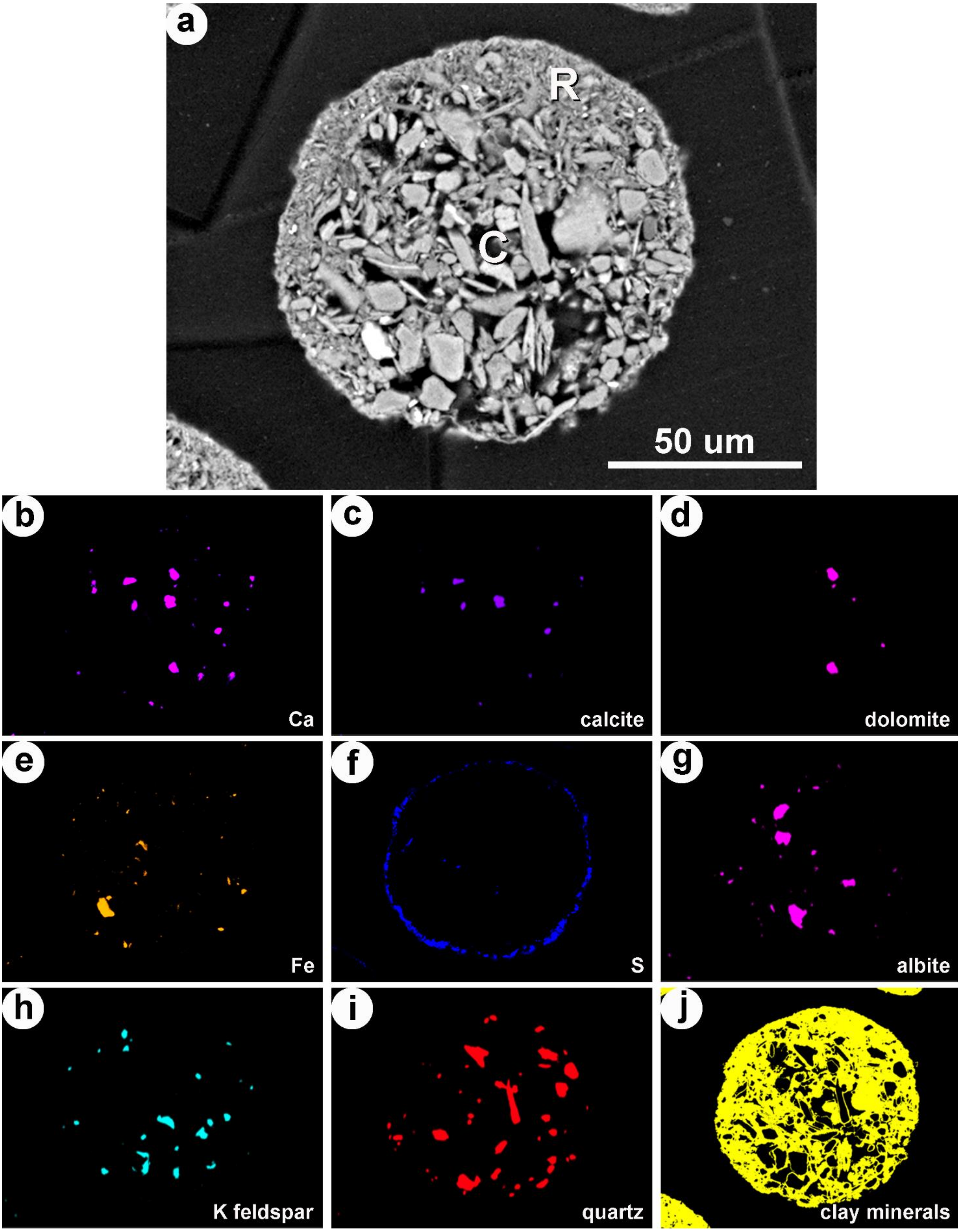

Fig. 6. VPSEM-EDX study of sectioned iberulite (sampled in summer 2010) with spatial distribution of components. a) Retro-dispersed electron image; shape almost perfectly circular, diameter approx. 120 microns; core (C) and rind (R) can be observed; the vortex must be situated in direction N-NW in the image, as shown by thickening of rind (R). Maps of: b) Ca, c) calcite, d) dolomite, e) Fe, f) S, g) albite, h) k feldspar, i) quartz and j) clay minerals.

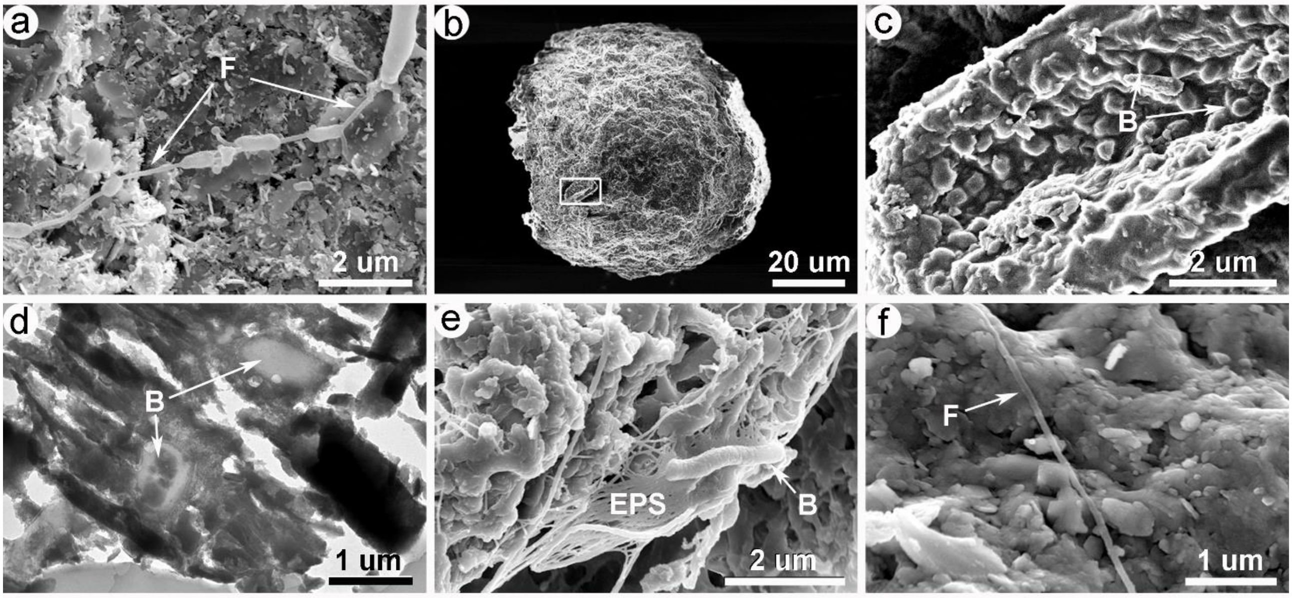

Fig. 7. Presence of bacteria and products of their activity (SEM and HRTEM images). **a)** Presence of chain of bacteria with filament (F) in upper horizon of a soil close to the sampling zone. **b)** Iberulite with unknown biological specimen adhering to it (shown by rectangle). **c)** Detail of b). Colonization of previous biological specimen by nanobacteria (B). **d)** HRTEM image of intact microbial cells (B) embedded in the clayey matrix of a polished section of an undyed iberulite. **e)** Aggregate of mineral particles in sample of atmospheric dust collected in "wet deposition" – "red rain". Bacterial biofilms (EPSs) cementing particles. **f)** Detail of surface of iberulite collected in "dry deposition". Very fine (pilum or flagellum) bacterial filament (F) which traverses and stabilizes the surface of the iberulite (similar to the "filaments" connecting the bacteria in microphotograph a). Images b), c) and d) are from samples collected by dry-deposition in summer 2015; image e), summer 2016 by wet-deposition; image f), summer 2010. All samples were taken in the sampling site.

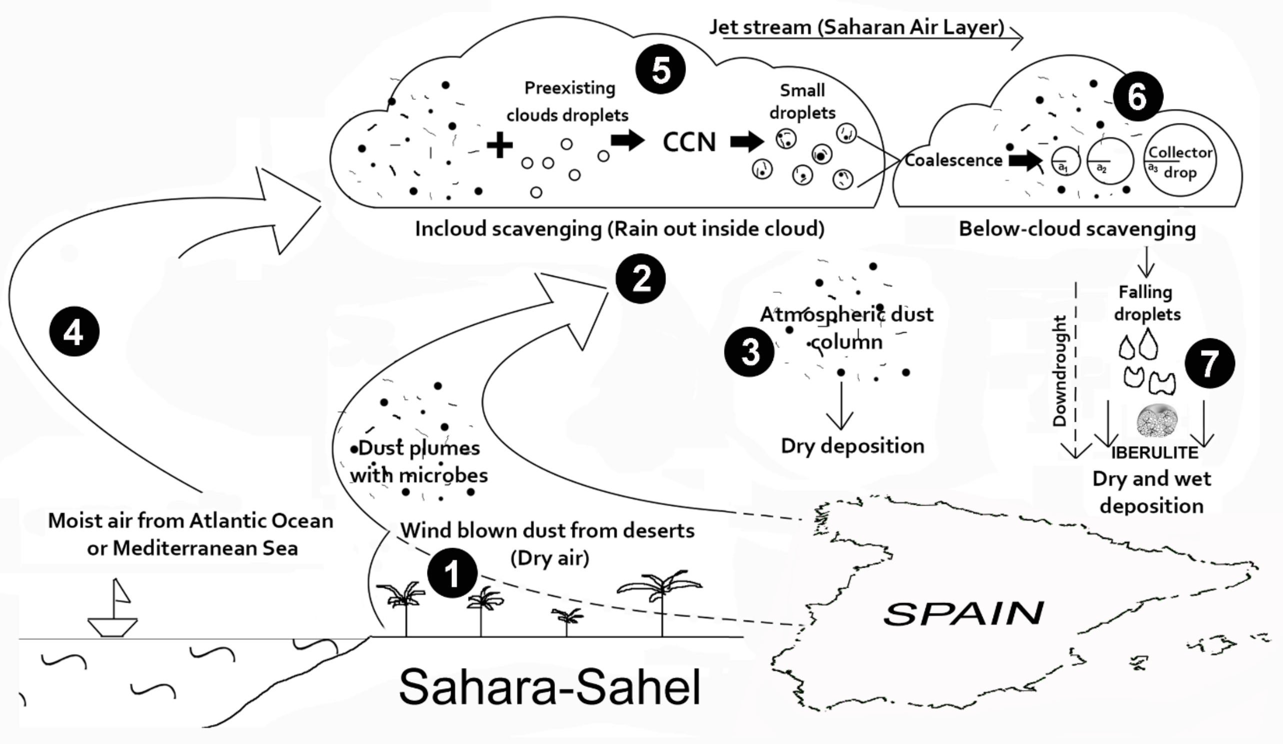

Fig. 8. Sequence of iberulite formation via "cloud processing" with bacterial activity. **1)** The wind picks up dust (mineral particles and bacteria) from the unvegetated surfaces of soils and sediments of African arid and semi-arid zones. Part of this dust may be from Spain. **2)** Ejection of fine particles and bacteria to altitude. **3)** Columns of suspended atmospheric dust which may fall (dry deposition). **4)** Saturated air rises into the atmosphere from the surface of marine water masses. **5)** Water droplets, dust particles and microbes coincide within the clouds. Formation of water droplets from cloud condensation nuclei –CCN-. **6)** Water droplets become collector droplets. Note increase in radius "a". Below-cloud scavenging. Simultaneous bacterial growth. **7)** Falling of droplets and formation of iberulite with bacterial assistance. Role of EPS cements between particles (Fig. 7.e) and stabilization of surface (Fig. 7.f).

Table 1. Granulometric characteristics. Deposited dust[a] and iberulites.

		Granulometric fraction (% volume)			Iberulites	
Sample	Sampling period	>500 µm	200 - 500 µm	<200 µm	% [b]	Mean apparent diameter (µm)
JP01	01/06/2010 - 03/07/2010	1.7	1.3	97.0	1.6	53
JP02	05/07/2010 - 12/07/2010	0.5	4.6	94.9	9.2	61
JP03	13/07/2010 - 20/07/2010	1.8	9.7	88.5	3.1	57
JP04	21/07/2010 - 27/07/2010	0.9	4.6	94.5	4.7	77
JP05	28/07/2010 - 02/08/2010	3.8	7.4	88.8	1.5	94
JP06	03/08/2010 - 10/08/2010	1.1	6.8	92.1	2.7	59
JP07	11/08/2010 - 17/08/2010	0.9	3.8	95.3	1.9	48
JP08	18/08/2010 - 24/08/2010	3.0	11.0	86.0	1.6	48
JP09	25/08/2010 - 31/08/2010	2.0	6.3	91.7	1.1	49
JP10	01/09/2010 - 08/09/2010	2.3	4.9	92.8	2.7	34
JP11	09/09/2010 - 15/09/2010	1.7	7.8	90.5	0.9	51
JP12	16/09/2010 - 29/09/2010	3.8	5.4	90.8	4.4	53
JP13	30/09/2010 - 14/10/2010	2.0	3.4	94.6	0.7	59
JP14	15/10/2010 - 31/10/2010	2.3	3.7	94.0	0.8	111

[a]Data obtained by laser granulometry (this study)
[b] Percentage of iberulites in particles observed

Table 2. Mineralogy (XRD) (%) of atmospheric dust sampled.

Sample	CM	1.0-1.5Ph	Il	Pa	Ka	Ch	Qz	FdK	Pl	Ca	Do	FeOx	Gy
JP01	31	2	22	5	2	3	13	<1	1	19	27	6	<1
JP02	40	5	17	9	9	1	29	<1	-	8	13	8	1
JP03	32	9	19	<1	4	1	16	tr	3	15	27	6	tr
JP04	48	6	26	5	11	1	16	2	<1	13	17	2	1
JP05	32	3	25	<1	4	4	25	tr	1	16	18	4	<1
JP06	56	8	31	10	7	2	14	1	-	9	15	2	1
JP07	44	9	19	6	10	1	21	2	3	8	16	5	<1
JP08	15	3	7	-	5	<1	64	tr	-	4	17	tr	<1
JP09	49	10	27	6	6	1	18	tr	2	15	15	<1	<1
JP11	43	9	19	8	7	1	26	<1	<1	10	20	<1	<1
JP12	37	5	28	<1	4	2	20	<1	-	11	25	5	<1
JP13	37	4	18	8	7	3	13	<1	<1	12	35	<1	<1
JP14	49	3	31	8	7	2	14	<1	<1	8	18	9	tr
Mean (SD)	39 (11)	6 (3)	22 (7)	5 (4)	6 (3)	2 (1)	22 (14)	1	1	11 (4)	20 (6)	4 (3)	1

CM: Clay Minerals *sensu* Schultz (1964) (all phyllosilicates except chlorite); 1.0-1.5Ph: mineral phases with reflections d_{00l} between 1.0 and 1.5 nm spacing (mainly mixed layers and smectites; without chlorite); Il: illite; Pa, paragonite; Ch: Chlorite; Ka: kaolinite; Qz: quartz; FdK: K feldspar; Pl: plagioclases; Ca: calcite; Do: dolomite; FeOx: iron oxides; Gy: gypsum.
Sample JP10 not included in this Table due to low quantity of dust.

Table 3. Mineralogical indices of atmospheric dust and soil samples.

	Location	Reference	Sample	Type of event	Period/year of event	Il/Ka[1]	Ch/Ka[1]	Palygorskite (%)[1]	Carbonates (%)[1]	Ca/Do
Atmospheric dust samples		this study	JP01 to JP14	DD	2010					
Mean (n=13)						4.25 (2)	0.38 (2,3,4)	nd (4,5,6)	32 (1,2,3)	0.58
SD						2.67	0.42		9	0.21
Max						11.00 (2)	1.50 (1,4)	nd (4,5,6)	47 (1,2,3)	1.00
Min						1.40 (1,2,4)	0.09 (2,4)	nd (4,5,6)	21 (1,2,3)	0.23
Other atmospheric dust samples from Iberian peninsula and Balearic Islands										
	Catalonia	Avila et al. (1997)	WS	RR	1984-1992	5.39 (2)	(5)	7.3 (1,2)	12 (3,4)	1.40
			MA	RR	1984-1992	11.26 (2)	(5)	10.1 (1,2)	17 (3,4)	2.19
			CA	RR	1984-1992	2.76 (2)	(5)	8.3 (1,2)	2 (5)	1.33
	Mallorca	Fiol et al. (2001)		WD	1988-1992	0.21 (1,4,5)	(5)	nd (4,5,6)	34 (1,2,3)	3.61
		Fiol et al. (2005)		WD	1989-1999	0.52 (1,3,4)	(5)	1.0 (3)	36 (1,2,3)	2.78
		Fornós et al. (2004)		RR	2004	1.07 (1,2,3,4)	(5)	6.0 (1,2)	25 (1,2,3)	4.83
		Fornós et al. (2004)		DD	2004		(5)	9.4 (1,2)	31 (1,2,3)	2.38
	Sierra Filabres	Queralt et al. (1993)		WD	1989-1990	5.93 (2)	1.47 (4)	3.7 (3)	2 (5)	0.60
	Granada	Díaz-Hernández and Párraga (2008)	dust	DD	2001-2005	2.40 (2)	(5)	nd (4,5,6)	51 (1,2,3)	0.20
			iberulite	DD	2001-2005	1.75 (1,2,4)	(5)	nd (4,5,6)	22 (1,2,3)	3.46
		Díaz-Hernández et al. (2011)	F1	DD	1992	0.89 (1,2,3,4)	0.46 (2,3,4)	(3)	26 (1,2,3)	0.91
			F2	DD	1992	1.06 (1,2,4)	0.46 (2,3,4)	(3)	30 (1,2,3)	0.61
			F3	DD	1992	0.33 (1,3,4,5)	0.38 (2,3,4)	(3)	22 (1,2,3)	2.65
		Rodríguez-Navarro et al. (2018)	bulk	RR	2017	3.36 (2)	(5)	11 (1,2)	23 (1,2,3)	4.50
			silt	RR	2017	1.68 (1,2,4)	0.32 (2,3,4)	10.7 (1,2)		
			clay	RR	2017	2.07 (2)	(5)	6.3 (1,2)		
Soils										
Entisols	Sierra Nevada	Martín-García et al. (2004)	coarse sand					nd (4,5,6)	nd (5)	
			fine sand					nd (4,5,6)	nd (5)	
			silt			18.34 (2)	1.00 (2,4)	nd (4,5,6)	nd (5)	
			clay			4.47 (2)	0.68	nd (4,5,6)	nd (5)	
Terrae rossae	Sierra Gádor	Delgado et al. (2003)	coarse sand					nd (4,5,6)	15 (3,4)	1.68
			fine sand					nd (4,5,6)	5 (3,5)	0.10
			silt			6.63 (2)	0.36 (2,3,4)	nd (4,5,6)	nd (5)	
			clay			6.95 (2)	0.16 (2,4)	nd (4,5,6)	nd (5)	
Mean soils	Granada	Márquez (2012)	coarse sand					nd (4,5,6)	24 (1,2,3)	1.14
			fine sand					nd (4,5,6)	24 (1,2,3)	1.27
			silt					nd (4,5,6)	19 (3,4)	2.10
			clay			3.18 (2)	0.49 (2,3,4)	nd (4,5,6)	10 (3,4)	7.50

DD: dry deposition; RR: red rain; WD: wet deposition; Il: illite; Ch: Chlorite; Ka: kaolinite; Ca: calcite; Do: dolomite; nd, not detected.

[1] Scheuvens et al. (2013) fingerprints. Numbers in brackets indicate the potential source areas in northern Africa: 1, Tunisia and northern Algeria (PSA1); 2, foothills of Atlas mountains and western coastal region (PSA2); 3, southern Algeria and northern Mali (PSA3); 4, central Libya (PSA4); 5, western Chad including Bodélé depression (PSA5); 6, southern Egypt and northern Sudan (PSA6).

Table S1. Contents of rare earth elements (ppm) in collected dust samples and comparison with literature.

Reference	sample	La	Ce	Pr	Nd	Sm	Eu	Gd	Tb	Dy	Ho	Y	Er	Tm	Yb	Lu	ΣLn	ΣLREE	ΣMREE	ΣHREE
This study	JP01	17.04	32.79	3.77	14.01	2.73	0.58	2.09	0.29	1.62	0.28	nd	0.73	0.10	0.63	0.11	76.77	67.61	7.31	1.85
	JP02	15.37	31.41	3.52	13.38	2.52	0.58	2.09	0.28	1.64	0.29	8.62	0.77	0.12	0.73	0.12	72.83	63.69	7.12	2.02
	JP03	11.39	21.86	2.49	9.40	1.80	0.42	1.44	0.18	1.10	0.19	6.13	0.49	0.07	0.44	0.07	51.34	45.14	4.94	1.26
	JP04	18.31	36.70	4.16	15.64	3.02	0.66	2.43	0.34	1.90	0.35	9.73	0.89	0.13	0.84	0.13	85.50	74.81	8.35	2.34
	JP05	12.95	25.30	2.88	10.89	2.11	0.49	1.68	0.22	1.42	0.23	7.02	0.62	0.09	0.56	0.09	59.53	52.02	5.92	1.59
	JP06	16.41	32.31	3.68	13.94	2.68	0.58	2.12	0.28	1.52	0.26	7.67	0.68	0.10	0.61	0.10	75.27	66.34	7.18	1.75
	JP07	16.00	36.99	3.66	13.54	2.58	0.58	2.06	0.28	1.62	0.28	7.88	0.76	0.12	0.69	0.11	79.27	70.19	7.12	1.96
	JP08	13.23	29.62	3.75	10.50	1.92	0.45	1.44	0.19	1.15	0.18	6.09	0.50	0.06	0.44	0.07	63.49	57.09	5.15	1.25
	JP09	13.46	27.14	3.19	10.97	2.06	0.46	1.63	0.21	1.25	0.23	6.57	0.57	0.08	0.49	0.08	61.82	54.76	5.61	1.45
	JP10	12.55	25.78	2.95	10.64	2.12	0.45	1.82	0.27	1.33	0.25	6.87	0.65	0.08	0.61	0.09	59.59	51.92	5.99	1.68
	JP11	17.52	35.95	3.66	13.36	2.63	0.55	2.19	0.33	1.68	0.31	7.95	0.80	0.11	0.71	0.10	79.90	70.49	7.38	2.03
	JP12	12.14	23.88	2.66	10.00	2.04	0.43	1.76	0.26	1.32	0.24	6.64	0.62	0.08	0.58	0.09	56.10	48.68	5.81	1.61
	JP13	13.96	27.86	3.11	11.81	2.38	0.49	2.02	0.29	1.45	0.26	nd	0.67	0.09	0.62	0.09	65.10	56.74	6.63	1.73
	JP14	13.45	25.21	2.91	10.68	2.18	0.44	1.89	0.27	1.44	0.25	nd	0.62	0.10	0.56	0.09	60.09	52.25	6.22	1.62
	mean (SD)	14.56 (2.19)	29.49 (4.96)	3.31 (0.49)	12.05 (1.88)	2.34 (0.36)	0.51 (0.08)	1.90 (0.29)	0.26 (0.05)	1.46 (0.22)	0.26 (0.04)	7.38 (1.12)	0.67 (0.11)	0.10 (0.02)	0.61 (0.11)	0.10 (0.02)	67.61 (10.44)	59.41 (9.30)	6.48 (0.97)	1.72 (0.30)
Hoggar Massif[1]	HM1	56.00	121.00	14.00	58.00	9.00	1.00	10.00	1.00	9.00	2.00	39.00	4.00	1.00	5.00	1.00	249.00	30.00	13.00	249.00
	HM2	61.00	137.00	16.00	64.00	11.00	1.00	12.00	2.00	10.00	2.00	50.00	5.00	1.00	6.00	1.00	278.00	36.00	15.00	278.00
Chad[1]	CB1	45.00	94.00	11.00	48.00	6.00	2.00	9.00	1.00	7.00	1.00	19.00	3.00	1.00	3.00	0.25	198.00	25.00	8.25	198.00
	CB2	28.00	54.00	7.00	28.00	4.00	1.00	5.00	1.00	4.00	1.00	17.00	2.00	0.25	2.00	0.25	117.00	15.00	5.50	117.00
Niger[1]	MON	47.00	104.00	11.00	53.00	8.00	1.00	10.00	1.00	9.00	1.00	23.00	4.00	1.00	4.00	1.00	215.00	29.00	11.00	215.00
	HAR	46.00	99.00	11.00	50.00	8.00	2.00	9.00	1.00	8.00	1.00	22.00	4.00	1.00	4.00	1.00	206.00	28.00	11.00	206.00
Western Sahara[1]	WS1	35.00	75.00	8.00	37.00	6.00	1.00	7.00	1.00	6.00	1.00	17.00	3.00	0.25	3.00	0.25	155.00	21.00	7.50	155.00
	WS2	25.00	51.00	6.00	27.00	4.00	1.00	5.00	1.00	5.00	1.00	12.00	2.00	0.25	2.00	0.25	109.00	16.00	5.50	109.00
	WS3	56.00	124.00	14.00	62.00	9.00	1.00	11.00	1.00	8.00	2.00	27.00	4.00	1.00	5.00	1.00	256.00	30.00	13.00	256.00
Spanish Top-soil[2]		38.83	81.27	9.80	34.96	6.49	1.12	5.40	0.71	3.91	0.73	20.01	2.01	0.29	1.85	0.27	164.86	17.63	5.15	164.86
European Top-soil[3]		25.86	52.25	6.02	22.41	4.28	0.85	4.20	0.64	3.58	0.72	22.74	2.10	0.31	2.09	0.31	106.54	13.56	5.52	106.54
African dust[4]	<2 µm	61.00	133.00		57.10	11.50	2.31	11.40	1.35		1.62				3.69	0.54				
	2-5 µm	48.40	104.00		49.70	9.64	2.00	10.20	1.16		1.41				3.45	0.52				

5-10 µm	44.20	90.20		42.90	8.43	1.64	9.19	1.19		1.58				4.33	0.62
10-20 µm	46.60	94.90		45.70	8.96	1.77	9.48	1.34		1.95				5.81	0.85

LREE: light rare earth elements (La, Ce, Pr, Nd); MREE: medium rare earth elements (Sm, Eu, Gd, Tb, Dy); HREE: heavy rare earth elements (Ho, Er, Tm, Yb, Lu); nd: not determined

[1]Materials from Sahara-Sahel corridor (Moreno et al., 2006)

[2] Locutura et al. (2012)

[3] Salminen et al. (2005)

[4] Muhs et al. (2010)

Table 4. Geochemical indices of REE from samples of atmospheric dust studied and other materials.

Reference		$HREE_N/LREE_N$	$MREE_N/LREE_N$	Ce/Ce*	Eu/Eu*	Y/Y*
Atmospheric dust (this study)						
JP01		0.11	0.18	0.99	0.74	nd
JP02		0.13	0.19	1.03	0.77	1.09
JP03		0.11	0.18	0.99	0.80	1.20
JP04		0.13	0.19	1.02	0.74	1.04
JP05		0.13	0.19	1.00	0.79	1.11
JP06		0.11	0.18	1.01	0.74	1.09
JP07		0.12	0.18	1.17	0.77	1.02
JP08		0.09	0.15	1.02	0.82	1.21
JP09		0.11	0.17	1.00	0.77	1.08
JP10		0.13	0.20	1.03	0.70	1.01
JP11		0.12	0.18	1.09	0.70	0.95
JP12		0.13	0.21	1.02	0.69	1.02
JP13		0.12	0.20	1.02	0.68	nd
JP14		0.13	0.20	0.97	0.66	nd
Spanish Top-soil (Locutura et al., 2012)		0.10	0.17	1.01	0.58	0.98
European Top-soil (Salminen et al., 2005)		0.17	0.22	1.01	0.61	nd
Materials from Sahara-Sahel corridor (Moreno et al., 2006)						
Hoggar Massif	HM1	0.24	0.19	1.05	0.32	0.82
	HM2	0.23	0.22	1.06	0.27	0.94
	$mean_{Macizo\ Hoggar}$	0.24	0.21	1.06	0.30	0.88
Chad	CB1	0.19	0.24	1.02	0.83	0.65
	CB2	0.19	0.25	0.93	0.68	0.72
	$mean_{Cuenca\ del\ Chad}$	0.19	0.25	0.98	0.76	0.69
Niger	MON	0.25	0.22	1.11	0.34	0.68
	HAR	0.26	0.24	1.06	0.72	0.65
	$mean_{Níger}$	0.26	0.23	1.09	0.53	0.67
Western Sahara	WS1	0.17	0.24	1.08	0.47	0.58
	WS2	0.20	0.29	1.01	0.68	0.51
	WS3	0.24	0.18	1.07	0.31	0.57
	$mean_{Sahara\ Oeste}$	0.20	0.24	1.05	0.49	0.55
$mean_{Sahara-Sahel}$		0.22	0.23	1.04	0.51	0.68
African dust (Muhs et al., 2010)						
<2 µm					0.61	
2-5 µm					0.61	
5-10 µm					0.57	
10-20 µm					0.59	

nd: not determined

Click here to access/download
RDM Data Profile XML
DataProfile_4918955.xml

Declaration of interests

☒ The authors declare that they have no known competing financial interests or personal relationships that could have appeared to influence the work reported in this paper.

☐The authors declare the following financial interests/personal relationships which may be considered as potential competing interests:

Authors contributions:

J. Párraga, J.M. Martín-García, G. Delgado, A. Molinero-García, A. Cervera Mata, M.V. Fernández-González, F.J Martín-Rodríguez and R. Delgado have sampled and analyzed (mineralogical composition, REE contents, particle size distribution) the dust samples, iberulites and soils and described the biological contributions to the genesis of iberulites. H. Lyamani, J.A. Casquero-Vera, A. Valenzuela and F.J. Olmo have analyzed the atmospheric conditions of desert dust intrusions over the study area in summer 2010, the backtrajectory analysis computed by the HYSPLIT model, the PM concentrations and data of air quality and meteorological stations. I. Guerra has described the electronic micromorphology and microanalysis, of iberulites collected, by SEM-EDX and VPSEM-EDX. All authors wrote the manuscript.